Origin and fate of hydrothermal fluids at Piton des Neiges volcano (Réunion Island): A geochemical and isotopic (O, H, C, Sr, Li, Cl) study of thermal springs

Bhavani Bénard, Vincent Famin, Pierre Agrinier, Bertrand Aunay, Geneviève Lebeau, Bernard Sanjuan, Francoise Vimeux, Gérard Bardoux, Chrystel Dezayes

Origin and fate of hydrothermal fluids at Piton des Neiges volcano (Réunion Island): a geochemical and isotopic (O, H, C, Sr, Li, Cl) study of thermal springs

Bhavani Bénard[ab] (corresponding author), Vincent Famin[a], Pierre Agrinier[c], Bertrand Aunay[b], Geneviève Lebeau[a], Bernard Sanjuan[d], Françoise Vimeux[e], Gérard Bardoux[c], Chrystel Dezayes[d]

[a] Laboratoire GéoSciences Réunion, Université de La Réunion, Institut de Physique du Globe de Paris, Sorbonne Paris Cité, Université Paris Diderot, UMR 7154 CNRS, F-97744 Saint Denis, La Réunion

[b] BRGM, F-97417 Saint-Denis de La Réunion, France

[c] Institut de Physique du Globe de Paris, Université Sorbonne Paris Cité, Université Paris Diderot, CNRS, UMR 7154, 75005, Paris, France

[d] BRGM, F-45060 Orléans, France

[e] Institut de Recherche pour le Développement, Laboratoire HydroSciences Montpellier (UMR 5569) et Laboratoire des Sciences du Climat et de l'Environnement (UMR 8212), CEA Saclay, Orme des Merisiers, 91191 Gif-sur-Yvette Cedex, France

Contacts: bhavani.benard@univ-reunion.fr, vincent.famin@univ-reunion.fr, agrinier@ipgp.fr, b.aunay@brgm.fr, genevieve.lebeau@univ-reunion.fr, b.sanjuan@brgm.fr, francoise.vimeux@lsce.ipsl.fr, bardoux@ipgp.fr, c.dezayes@brgm.fr

Declarations of interest: none

Abstract

As many ocean basaltic volcanoes worldwide, Piton des Neiges (Réunion Island) hosts a hydrothermal system that represents a potential geothermal resource. Despite several prospection campaigns over the past decades, this potential has never been confirmed because many aspects of fluid supply and circulation remain unclear. To track the origin and fate of hydrothermal fluids, we analyzed the geochemistry of thermal springs (water and gas), by combining conventional tracers (major-trace elements and O, H, C, Sr, Li isotopes) with Cl

isotopes, a geochemical tool under development. Added to literature data, our new results allow us to compare the composition of thermal springs with cold waters, rocks, gas, and fumarolic deposits from La Réunion and elsewhere, and to untwine the complex history of fluid mixing that constitutes the geothermal system of Piton des Neiges.

$\delta^{18}O_{H2O}$ and δD_{H2O} values of springs (-8.67 to -4.9 and -56.3 to -23.5 ‰ VSMOW, respectively) are positioned close to the local meteoric water line, showing that thermal waters are of meteoric origin. However, their depletion in heavy isotopes relative to cold waters suggests a recharge strongly influenced by cyclones, with a possible contribution from high altitude (≥ 2000 m) rainfalls. Their absence of ^{18}O enrichment relative to the local meteoric water line indicates that the isotopic exchange between rocks and water is very limited, and therefore suggests that their deep temperatures are relatively low and/or the water/rock ratios are high. $\delta^{13}C$ values in thermal waters (-8.0 to +3.2 ‰ PDB) and gases (-6.7 to -5.3 ‰ PDB) confirm that carbon is essentially of magmatic origin, which we interpret as supplied by regional degassing of La Réunion hotspot. Major-trace elements and $^{87}Sr/^{86}Sr$ (0.704142 to 0.704336), $\delta^{7}Li$ (+2 ‰ and +34.8 ‰ LSVEC), and $\delta^{37}Cl$ (-0.35 ‰ and +0.40 ‰ SMOC) compositions show that three additional processes contribute to the mineralization of thermal waters: 1) interaction with basalt at temperatures ≥50 °C, 2) very limited seawater contamination (< 3 mol%), and/or 3) leaching of trachyte or scrubbing of fumarolic gas or condensates emitted by a shallow trachytic magma in the volcanic edifice.

The geothermal system of Piton des Neiges is thus the result of meteoric water interaction with a trachytic heat source (as a solidified intrusion or a magma pocket), unrelated to the CO_2 flux. We also emphasize that thermal waters at Piton des Neiges are exceptionally isolated from seawater compared to other geothermal systems in ocean island volcanoes worldwide, which implies a heat source located above the seawater/freshwater interface. These inferences are of critical importance for the future geothermal exploration on the island, as they suggest that the geothermal resource is within reach of relatively shallow drilling depths (≤ 1000 m).

Keywords: Piton des Neiges, Réunion Island; Ocean island volcano; Thermal springs; Hydrothermal system; Geothermal exploration; Major and trace elements; Isotope chemistry; Chlorine isotopes

1. Introduction

Ocean island basaltic volcanoes are among the most prized geological settings for geothermal exploitation, because they cumulate the advantages of a shallow and significant heat source, almost unlimited water supply, and low concentrations of toxic or radioactive elements in waters compared to granitic or andesitic settings. Iceland, Sao Miguel (Azores), Big Island (Hawaii) and

Pantelleria (Italy) are emblematic examples of such basaltic islands being exploited or showing potential for geothermal energy (Bertani, 2005; Gianelli and Grassi, 2001). However, ocean island volcanoes are also renowned for the complexity of their geothermal systems, seldom matching the ideal case of a heat source/reservoir/cap rock superposition as in the model of Johnston et al., (1992). This complexity requires case-by-case studies of fluid sources and pathways, which often discourages geothermal prospection or exploitation.

The island of La Réunion illustrates this difficulty of evaluating the geothermal potential of ocean island basaltic volcanoes. Réunion Island is made of two edifices, Piton de la Fournaise which is among the most active volcanoes of the world, and Piton des Neiges presently in a dormant state since 12 to 29 ka (Delibrias et al., 1986; Deniel et al., 1992; Gillot and Nativel, 1982). Piton des Neiges displays ample evidence of hydrothermal activity, including thermal springs (up to 50 °C for the hottest), fumarole deposits, and CO_2 – He – Rn anomalies (Marty et al., 1993; Rançon and Rocher, 1985; Sanjuan et al., 2001). Between 1980 and 2005, exploration campaigns of geophysics and drillings demonstrated the presence of dense intrusive complexes beneath Piton des Neiges, and temperature gradients locally exceeding 90 °C/km (see Dezayes et al., (2016) for a review). Using chemical and isotope geothermometers, geochemical studies also revealed the temperature of water-rock interaction ranged from 100 to 160°C for most of the thermal springs, (Lopoukhine and Stieltjes, 1978; Sanjuan et al., 2001). Despite these promising indicators, prospection did not fully succeed in locating and quantifying the resource of Piton des Neiges, partly because of the complex structure of this polygenic volcano, but most of all because of the difficulty of identifying multiple fluid reservoirs and pathways from the geochemical tools and data available at that time.

The objective of this paper is to improve our understanding of Piton des Neiges' hydrothermal system, by untangling the contribution of each fluid pool and the mixing and heating history of these fluids. The adopted strategy is to widen the geochemical description of thermal waters by applying proven and newly-developed tracers, and to increase the number of analyzed springs compared to previous studies. Our new results are combined with literature data into an exceptionally large geochemical set of major, trace elements and O, H, C, Sr, Li and Cl isotopes analyses of thermal springs from Piton des Neiges. Compared with the chemistry of rocks, seawater, cold waters, and fumarolic products from Réunion as well as from other similar geological contexts, this large dataset allows us to untwine the complex history of fluids at the origin of Piton des Neiges' hydrothermal system. The proposed circulation model may be used as a predictive tool for geothermal exploration in Réunion and other basaltic islands.

2. Geological and hydrogeological settings

Piton de la Fournaise and Piton des Neiges are often considered as analogue volcanoes with a similar structure and evolution, the former being in its shield building stage while the latter is at the end of its lifetime. Piton des Neiges is estimated to have emerged at ~3 Ma and has produced transitional basic magmas until 430 ka (Kluska, 1997; McDougall, 1971). After a 80 ka period of repose, the volcano entered into a differentiated stage 350 ka ago and produced alkali magmas ever since (Gillot and Nativel, 1982; Kluska, 1997). The terminal volcanism of Piton des Neiges began at about 210 ka, with the emission of higly differentiated magmas such as trachytes and syenites. The last known eruption of Piton des Neiges dates back to 12 ka (U/Th), 22 ka (^{14}C) or 29 ka (K/Ar), depending on the radiometric dating technique (Delibrias et al., 1986; Deniel et al., 1992; Gillot and Nativel, 1982).

Since its last activity, the heavy rainfalls under tropical climate have favored erosion of the volcanic edifice, now incised by three cirques (subcircular depressions), Salazie to the north, Mafate to the northwest, and Cilaos to the south (Figure 1). These deep cirques have dissected the inner structure of the volcano, erasing most of the surface evidence of calderas. Based on patchy observations of faults, offset lava layers, pyroclastic deposits or radial dykes, two calderas have been proposed: a large one running through the three cirques formed at the beginning of the terminal stage (210 – 180 ka), and a smaller one in the summit area of Piton des Neiges formed during its last activity (Figure 1). On the other hand, erosion has exposed the hypovolcanic complex, made of dense gabbroic plutons and basaltic, trachytic and syenitic planar intrusions. Planar intrusions are organized into two rift zones N030-40 and N120-160, and two sill zones between 800 and 1300 m above sea level (Chaput et al., 2017, 2014). Syenite intrusions, which consist in 30 – 100 m thick dykes in the cirques of Cilaos and Salazie, are of particular importance for the present study for two reasons: (1) they represent major dyke structures of the terminal volcanic activity, since they are located within the N030 rift zone, and are also interpreted to delineate the largest caldera at 210 – 180ka (Chevalier, 1979; Rocher, 1988); (2) because many thermal springs are found in their vicinity, syenite dykes might be associated with the heat source of the hydrothermal system, or at least with the fracture network enabling fluid circulation.

The hypovolcanic complex of Piton des Neiges is also affected by several phases of low-grade metamorphism and hydrothermal alteration (Chevalier, 1979; Rançon, 1985), resulting in the secondary precipitation of phrenite-pumpellyite facies minerals in rocks of the shield-building stage, followed by carbonate precipitation in differentiated rocks as well as in basic rocks (Famin et al., 2016). This long history of construction and destruction, intrusive activity and secondary mineral precipitation strongly affects the hydrogeology of Piton des Neiges, by limiting the escape of freshwater toward the sea and its downward infiltration in the lowermost, oldest and most impermeable rock units (Join et al., 2005; Violette et al., 1997).

The tropical climate of Réunion Island consists in a dry season (April-November), and a wet season (December-March) that delivers huge precipitation rates (annual average of ~ 2500 mm in the cirques). Most of these wet season rainfalls occur as cyclones (five events per year in average for the period 1981 – 2010; Jumaux et al., 2011), providing ample meteoric water to feed a hydrothermal system. However, the hydrothermal system of Piton des Neiges may be also alimented by seawater, as in the case of many other volcanic islands (Adams, 1996; Arnórsson, 1995a, 1995b; Carvalho et al., 2006; Druecker and Fan, 1976; Thomas, 1984). To date, no hydrogeological model explicitly accounts for the recharge of the deep thermal aquifers, and the relative contribution of seawater and meteoric water to the hydrothermal system remains to be evaluated.

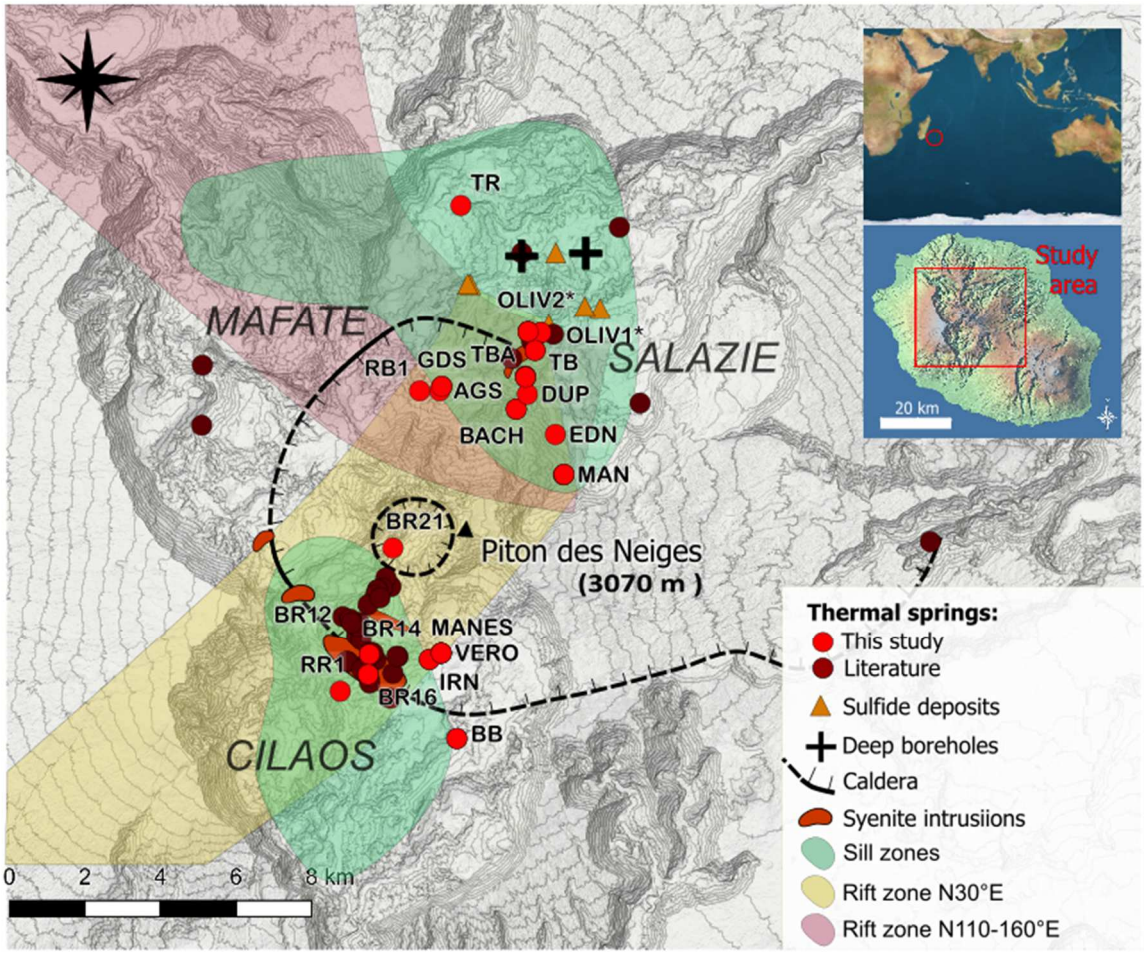

Figure 1: Location of thermal springs in Piton des Neiges, Réunion Island. Springs sampled for this study are labeled. Sulfide deposits (Lopoukhine and Stieltjes, 1978; Rançon and Rocher, 1985), proposed calderas (Chevalier, 1979), syenite intrusions, and rift and sill zones (Chaput et al., 2017) are also represented. Most springs are located in the cirques of Salazie and Cilaos. Map in UTM coordinates (EPSG:2975, RGR92 / UTM 40s, relief contours at 100 m intervals) from RGE ALTI® - IGN.

3. Methods

Thermal springs were sampled during two campaigns, the first one in June 2015 and the second one from December 2015 to January 2018. These campaigns yielded a total of twenty-seven water samples and seven gas samples of eighteen springs, to be analyzed for major, trace elements and O, H, Sr, Li, Cl and/or C isotopes (See Table B.1 for coordinates). Additionally, sixteen archive spring and river samples from Sanjuan et al. (2001) were analyzed for Li concentration, δ^7Li and δ^{37}Cl. During each sampling, the pH, temperature, and electrical conductivity (EC) of water were measured at the spring outlet. pH and EC are expressed at the *in situ* water temperature. For major, trace elements and Sr, Li, Cl isotope analyses, water samples were collected in HDPE bottles after filtration at 0.2 µm on site. For O and H isotope analyses, water was mainly sampled in amber glass bottles with cone shaped caps to avoid any isotopic exchange with ambient air, except during the first campaign (HDPE bottles). During the second campaign, water samples were also collected for analysis of total dissolved inorganic carbon content (TDIC) and C isotopes in Labco 12 ml Exetainer vials with no headspace. For all the water samples, the bottles were rinsed three times with filtered water from the sampled spring. Water samples for analysis of major cations and trace elements were acidified with nitric acid (HNO_3 0.3N) on site. Water samples for other analyses were not acidified. All samples were stored at a temperature of 6 °C before shipment.

The seven gas samples were collected during the second campaign at three springs, Irénée (IRN), Manès (MANES) and Véronique (VERO), used to supply a spa and a bottled water factory. For each spring, waters are channeled through a pipe (<50 m) to a glass dome, from where the supply line goes. A small opening on top of each dome provides access to the spring gas without atmosphere contamination. The free gas was channeled through a rubber pipe to a basin filled with water from the sampled spring. Underwater, the free gas was liberated as bubbles in an upside down Exetainer vial, thus replacing the water. Gas samples were analyzed for C isotopes only.

For the water samples of the first campaign, alkalinity, element and isotope analyses were performed at the Bureau de Recherches Géologiques et Minières (BRGM) in Orléans. For samples of the second campaign, total dissolved inorganic carbon (TDIC), major elements, C isotopes (water and gas) and Cl isotopes were performed at the Institut de Physique du Globe de Paris (IPGP). Oxygen and H isotopes analyses were performed at the Laboratoire des Sciences du Climat et de l'Environnement (LSCE) in Saclay. Trace elements and Sr isotope analyses were performed by the Service d'Analyse des Roches et des Minéraux (SARM-CRPG) in Nancy.

TDIC analyses from the second campaign were made by gas chromatography and isotope ratio mass spectrometry (GC-IRMS), after releasing TDIC as CO_2 by H_3PO_4 acidification in the case of water samples (Assayag et al., 2006). Concentrations for each carbonate species in

dissolved state were computed, either using alkalinity and pH (first campaign) or TDIC and pH (second campaign), depending on which data were available. In the case of the first campaign samples, alkalinity was determined using potentiometric titration.

Major anions and Br concentrations were determined by ion exchange chromatography. Major cations concentrations were determined using atomic emission spectrometry (ICP). Fluoride concentrations were obtained using ion exchange chromatography for the first campaign and by direct potentiometric determination for the second campaign. Lithium concentrations were obtained by ion exchange chromatography for the first campaign and by atomic absorption spectrometry for the second campaign. Boron concentrations were obtained by inductively coupled plasma mass spectrometry (ICP-MS) for the first campaign and UV-visible spectroscopy for the second campaign. Other trace element concentrations were determined by ICP-MS for the two campaigns.

Carbon isotope ratios were determined together with TDIC by GC—IRMS. Oxygen and H isotope ratios were also obtained by GC-IRMS, after equilibration with a gas (H_2 for hydrogen and CO_2 for oxygen) for the first campaign. For the second campaign, Oxygen and H isotopes were obtained using the CO_2-H_2O equilibration method on a Finnigan Mat 252 and the WS-CRDS infrared laser method respectively. Strontium isotope ratios were determined by mass spectrometry using a triple multidynamic acquisition and a single W filament for the first campaign, and by multi-collector mass spectrometry (TIMS) for the second campaign. Precisions are comprised between 0.000006 and 0.000018. Lithium isotope analyses were performed according to techniques detailed in Millot et al., (2004). Samples were prepared in order to obtain 60 ng of purified Lithium. Lithium was then separated from its matrix by ion exchange chromatography. The absence of isotopic fractionation during the purification procedure was tested by repeated analysis of the seawater standard IRMM BCR-403. The isotopic composition of Lithium was then obtained by ICP-MS using the "standard-bracketing" method and blank-corrected for the sample environment (HNO_3 3%) and instrumental background noise. Chlorine isotope analyses were performed according to techniques previously detailed (Bonifacie et al., 2007; Godon et al., 2004). Because the minimum Cl concentration for high quality isotopic analyses is ~10 mg/L, we restricted our analyses to springs above this limit. Chloride from water samples were converted to CH_3Cl with the following technique (Eggenkamp et al., 1994): chlorides were completely precipitated as AgCl and immediately filtrated, protected from light, and dried overnight in an oven at 80 °C, without pre-concentration. The dried filter was loaded into a pyrex tube with excess CH_3I, sealed under vacuum and reacted at 80 °C for 48 hours. The tube was then cracked under vacuum and the CH_3Cl product was separated from the excess CH_3I by gas chromatography (2 columns filled with porapak Q). The clean CH_3Cl was finally quantified

by a Baratron® pressure gauge, collected in sample tube and transferred to a dual inlet isotopic ratio mass spectrometer for Cl isotope analysis.

Non radiogenic isotope ratios are given using the δ notation, $\delta^{18}O_{H2O}$ and δD_{H2O} values being expressed with respect to VSMOW, and $\delta^{13}C$, $\delta^{7}Li$, and $\delta^{37}Cl$ being reported relative to PDB, LSVEC, and SMOC standards, respectively. Precisions are 0.05‰ VSMOW, 0.7‰ VSMOW, 0.1 ‰ PDB, 0.5 ‰ LSVEC, and 0.05 ‰ SMOC respectively.

4. Results

New analyses of major and trace element concentrations, and O-, D-, Sr, Li- and Cl isotopes are presented in Table 1 and Table 2. TDIC and C isotope data are reported in Table 3. An extensive compilation of literature data for thermal springs and cold waters in La Réunion is also provided in Supplementary Material. The most important results are also summarized in Figure 1 to Figure 6.

Table 1: Major elements concentrations, C, O, H, Sr, Li and Cl isotope ratios in thermal springs of Piton des Neiges analyzed in this study. (See Table B.1 for a compilation of data from previous studies)

Spring	Date	Electrical Conductivity (µS/cm)	pH	Temperature (°C)	Ca (mmol/L)	Mg (mmol/L)	Na (mmol/L)	K (mmol/L)	HCO_3 (mmol/L)	SO_4 (mmol/L)	Cl (mmol/L)	SiO_2 (mmol/L)	CO_3 (mmol/L)	NH_4 (mmol/L)	NO_2 (mmol/L)	NO_3 (mmol/L)	$\delta^{18}O$ (‰ VSMOW)	δD (‰ VSMOW)	$^{87}Sr/^{86}Sr$	δ^7Li (‰ LSVEC)	$\delta^{37}Cl$ (‰ SMOC)
AGS	17/06/2015	1746	6.5	21.1	6.8	3.5	1.7	0.1	14.5	4.1	0.0	1.3	b.d.l.	b.d.l.	b.d.l.	b.d.l.				9.1	
BACH	15/06/2015	1260	6.9	25.6	2.9	2.6	3.9	0.1	14.4	0.1	0.1	1.3	b.d.l.	b.d.l.	b.d.l.	b.d.l.	-6.70	-41.6	0.704317	11.9	
BACH*	Sanjuan et al., 2001	1540	7.4	19.4	3.6	3.5	5.5	0.2	18.7	0.2	0.1	1.5		b.d.l.	b.d.l.	b.d.l.	-6.7	-37.2	0.704300	13[1]	
BB	05/05/2017	1699	6.7	25.1	4.1	3.3	5.9	0.1	18.1	2.3	0.4	2.0				0.01	-8.06	-53.1	0.704139		0.3
BB	Sanjuan et al., 2001	1610	6.7	22.6	4.2	3.4	5.5	0.1	15.4	2.1	0.3	1.9		b.d.l.	b.d.l.	b.d.l.	-8.2	-54.3	0.704142	18[1]	
BR12	Sanjuan et al., 2001	1430	6.3	36.3	1.6	1.3	10.8	0.3	11.6	2.1	0.6	2.1		b.d.l.	b.d.l.	b.d.l.	-8.2	-50.5	0.704162	2[1]	
BR14	08/09/2017	1764	6.8	37.2	1.5	2.5	12.4	0.3	24.7	0.9	1.2	2.5				b.d.l.	-8.53	-53.7	0.704179		-0.4
BR16	29/10/2017	3370	6.5	29.1	0.2	3.1	25.0	1.0	22.7	0.5	5.1	2.6				0.00	-8.67	-53.3	0.704162		0.0
BR16	30/07/2016	2530	6.8	25.9	0.4	2.4	18.4	0.9	21.7	0.4	3.2	2.0	0.01			b.d.l.	-8.41	-52.0	0.704165		0.1
BR21	23/08/2016	1256	6.2	25.1	1.8	0.6	9.8	0.1	7.4	0.5	0.4	0.6	0.00			b.d.l.	-8.07	-51.7	0.704249		0.4
DUP	15/06/2015	714	8.1	23.3	1.4	1.3	2.8	0.1	7.2	0.4	0.1	1.0	b.d.l.	b.d.l.	b.d.l.	b.d.l.	-6.50	-38.4	0.704224	13.3	
EDN	16/05/2015	1855	6.4	25.5	3.2	6.2	4.0	0.2	23.0	0.1	0.0	2.3	b.d.l.	b.d.l.	b.d.l.	b.d.l.	-6.50	-38.7	0.704237	9.6	
GDS	17/06/2015	1234	7.7	18.7	4.7	2.2	1.3	0.1	8.8	3.3	0.0	0.8	b.d.l.	b.d.l.	b.d.l.	b.d.l.	-5.90	-33.1	0.704330	14.5	
GDS	Sanjuan et al., 2001		6.6	18.6	4.6	2.2	1.3	0.1	8.4	2.9	0.1	0.7		b.d.l.	b.d.l.	b.d.l.	-4.9	-23.5	0.704336	16.6[1]	
IRN	05/05/2017	2510	6.5	35.1	0.4	4.2	15.0	0.2	0.0	1.0	0.2	2.3				0.00	-8.05	-51.0			
IRN	15/06/2017	2500	6.4	36	0.1	4.1	14.8	0.2	24.6	1.0	0.2	2.4				0.00	-8.10	-51.2	0.704168		
IRN	28/07/2017	2520	6.4	35.6													-8.09	-51.2			
IRN	30/08/2017	2560	6.4	36.2	0.1	4.2	15.5	0.2	29.0	1.0	0.2	2.4				0.00	-8.04	-50.9			
IRN	25/09/2017	2560	6.6	36.2	0.1	4.1	15.1	0.2	20.0	1.0	0.2	2.4				0.00	-7.89	-50.9			
IRN	26/10/2017	2570	6.4	34.3	0.1	4.3	15.3	0.2	25.3	1.0	0.2	2.4				0.00	-8.06	-51.0			
IRN	29/11/2017	2570	6.7		0.1	4.2	15.1	0.2	20.5	1.0	0.2	2.5				0.00	-8.14	-51.1	0.704181		
IRN	Sanjuan et al., 2001	2370	6.0	37.8	4.6	4.6	16.1	0.2	31.2	1.1	0.1	2.6		b.d.l.	b.d.l.	b.d.l.	-8.2	-51.3	0.704169	12[1]	
MAN	16/06/2015	1395	6.6	30.6	3.3	2.7	4.4	0.2	16.6	0.1	0.1	1.8	b.d.l.	b.d.l.	b.d.l.	b.d.l.	-7.20	-43.4	0.704273	10.0	
MAN	Sanjuan et al., 2001	1580	6.6	30.6	4.1	3.4	5.0	0.2	19.2	0.1	0.1	2.0		b.d.l.	b.d.l.	b.d.l.	-7.6	-43.9	0.704282	8[1]	
MAN G	Sanjuan et al., 2001	1333	7.9	19	4.0	3.0	2.7	0.1	15.8	0.1	0.0	1.6		b.d.l.	b.d.l.	b.d.l.	-7.0	-39.8		7.5[1]	
MANES	15/06/2017	2310	6.4	29.8	0.3	3.9	13.0	0.2	22.1	0.9	0.2					0.00	-8.04	-51.5			
MANES	Sanjuan et al., 2001	2260	5.3	31	4.0	4.1	12.9	0.2	26.7	0.8	0.1	2.1		b.d.l.	b.d.l.	b.d.l.	-8.2	-54.3		15.7[1]	
OLIV1	Sanjuan et al, 2001	994	7.3	18.9	1.4	1.3	5.7	0.1	8.2	0.5	1.4	0.7	b.d.l.	b.d.l.	b.d.l.	-4.5	-6.5	-40.1		11.6[1]	0.08[1]
OLIV2	Sanjuan et al, 2001	4980	6.1	26	4.1	4.6	47.0	0.5	42.7	3.2	12.9	0.8	b.d.l.	b.d.l.	b.d.l.	1.8	-7.8	-45.9	0.704270	34.8[1]	0.06[1]
PISSA	Sanjuan et al., 2001	1190	6.7	18.4	4.4	1.4	3.1	0.0	11.6	1.3	0.0	1.3		b.d.l.	b.d.l.	b.d.l.	-6.7	-41.4		11.1[1]	
RB1	15/10/2016	929	6.0	19.8	1.0	1.8	1.2	0.2	7.9	0.1	0.1	1.6	0.00			b.d.l.	-6.50	-37.1	0.704308		
RFOUQ	Sanjuan et al., 2001	1000	7.4	19.2	2.9	2.3	2.2	0.0	11.3	0.3	0.0	0.7		b.d.l.	b.d.l.	b.d.l.	-6.5	-37.9		21.8[1]	
RR1	30/07/2016	1586	6.2	32.5	0.6	1.4	10.3	0.3	7.4	0.9	1.5	1.8	0.00			b.d.l.	-8.48	-56.3	0.704167		0.2
sRMAT	Sanjuan et al., 2001		7.9	18	1.9	6.0	3.7	0.3	17.7	0.5	0.1	1.2		b.d.l.	b.d.l.	b.d.l.	-5.9	-36.5		12[1]	
sRMAT2	Sanjuan et al., 2001	716	7.1	21.2	1.9	1.4	1.9	0.1	8.2	0.1	0.1	0.5		b.d.l.	b.d.l.	b.d.l.	-6.2	-35.5		13[1]	
sRMAT3	Sanjuan et al., 2001	1380	7.4	26.1	3.5	2.8	9.6	0.2	15.6	2.8	0.3	1.9		0.11	b.d.l.	b.d.l.				20.6[1]	
TB	22/11/2017	1410	6.3	34.4	1.2	1.0	9.4	0.3	12.0	0.6	0.7	1.1				b.d.l.	-6.42	-38.7	0.704194		0.3

Spring	Date	Electrical Conductivity (µS/cm)	pH	Temperature (°C)	Ca (mmol/L)	Mg (mmol/L)	Na (mmol/L)	K (mmol/L)	HCO_3 (mmol/L)	SO_4 (mmol/L)	Cl (mmol/L)	SiO_2 (mmol/L)	CO_3 (mmol/L)	NH_4 (mmol/L)	NO_2 (mmol/L)	NO_3 (mmol/L)	$\delta^{18}O$ (‰ VSMOW)	δD (‰ VSMOW)	$^{87}Sr/^{86}Sr$	δ^7Li (‰ LSVEC)	$\delta^{37}Cl$ (‰ SMOC)
TBA	15/06/2015	1718	6.3	26.6	4.0	2.5	7.1	0.2	17.0	1.0	0.1	2.1	b.d.l.	b.d.l.	b.d.l.	b.d.l.				11.5	
TR	21/07/2017	379	7.3	20.8	0.8	0.8	0.7	0.0	3.1	1.1	0.1	0.5				0.00	-6.69	-41.1	0.704333		
TR	30/01/2018	1016	7.5	20.8	2.4	2.7	1.1	0.1	4.2	5.1	0.1	0.6				0.00			0.704308		
VERO	15/06/2017	1938	6.2	29.5	0.2	3.3	10.6	0.2	20.8	0.7	0.1					0.00	-7.96	-51.6			
VERO	30/08/2017	1986	6.2	29.7	0.2	3.4	10.7	0.2	16.2	0.7	0.1					0.00	-7.96	-51.2			
VERO	Sanjuan et al., 2001	2010	5.4	30.3	3.6	3.7	10.9	0.1	23.5	0.7	0.1	2.0		b.d.l.	b.d.l.	b.d.l.	-8.1	-51.2		14.1[1]	

[1] $\delta^{37}Cl$ and δ^7Li data on samples from Sanjuan et al (2001) are from this study

Table 2: Trace elements concentrations in thermal springs of Piton des Neiges analyzed in this study. (See Table B.2 for a compilation of data from previous studies)

Spring	Date	Li (µmol/L)	Be (µmol/L)	B (µmol/L)	F (mmol/L)	Al (µmol/L)	P (mmol/L)	Ti (mmol/L)	V (µmol/L)	Cr (µmol/L)	Mn (µmol/L)	Fe (mmol/L)	Co (µmol/L)	Ni (µmol/L)	Cu (µmol/L)	Zn (µmol/L)	Ga (nmol/L)	As (µmol/L)	Rb (µmol/L)	Sr (µmol/L)	Y (µmol/L)	Ag (µmol/L)	Cd (µmol/L)	In (nmol/L)	Cs (µmol/L)	Ba (µmol/L)	La (nmol/L)	Pb (µmol/L)	Bi (µmol/L)	Ce (nmol/L)	Pr (nmol/L)	Nd (nmol/L)	Sm (nmol/L)	Eu (nmol/L)	Gd (nmol/L)	Tb (nmol/L)	Dy (nmol/L)	Ho (nmol/L)	Er (nmol/L)	Tm (nmol/L)	Yb (nmol/L)	Lu (nmol/L)	Th (µmol/L)	U (µmol/L)
AGS	17/06/2015	1.21	b.d.l.	0.83	0.01	0.03	b.d.l.			b.d.l.	4.19	0.00	0.01	0.22	0.01	b.d.l.		b.d.l.	0.18	15.72		b.d.l.	b.d.l.			0.06		b.d.l.																
BACH	15/06/2015	2.41	b.d.l.	2.81	b.d.l.	0.05	0.001			0.00	0.00	b.d.l.	b.d.l.	0.05	0.01	b.d.l.		0.00	0.22	8.00		b.d.l.	0.00			0.01		b.d.l.																
BACH	Sanjuan et al., 2001	2.88[1]		5.37	b.d.l.	b.d.l.				b.d.l.	b.d.l.	b.d.l.	b.d.l.	0.12	b.d.l.	b.d.l.		b.d.l.	0.27	10.39		b.d.l.	b.d.l.		b.d.l.	b.d.l.		b.d.l.																b.d.l.
BB	05/05/2017	1.17	b.d.l.	10.73	0.01	0.78	b.d.l.	b.d.l.	b.d.l.	b.d.l.	6.97	0.02	0.04	0.55	0.02	0.12	b.d.l.	b.d.l.	0.07	5.05	0.00		b.d.l.	b.d.l.	b.d.l.	0.00	0.03	0.00	b.d.l.	0.04	b.d.l.	b.d.l.	b.d.l.	b.d.l.	b.d.l.	b.d.l.	b.d.l.	b.d.l.	b.d.l.	b.d.l.	b.d.l.	b.d.l.	b.d.l.	0.00
BB	Sanjuan et al., 2001	1.01[1]		10.64	0.01	b.d.l.				b.d.l.	6.61	0.05	0.05	0.75	b.d.l.	b.d.l.		b.d.l.	0.06	5.48		b.d.l.	b.d.l.		b.d.l.	b.d.l.		b.d.l.																b.d.l.
BR14	08/09/2017	14.19	0.00	74.28	0.08	b.d.l.	b.d.l.	b.d.l.	0.02	0.03	b.d.l.	b.d.l.	b.d.l.	0.02	0.01	0.05	b.d.l.	0.04	1.03	10.50	0.00		b.d.l.	b.d.l.	0.01	0.02	b.d.l.	0.00	b.d.l.	0.06	b.d.l.	b.d.l.	b.d.l.	b.d.l.	b.d.l.	b.d.l.	b.d.l.	b.d.l.	b.d.l.	b.d.l.	b.d.l.	b.d.l.	b.d.l.	0.00
BR14	Sanjuan et al., 2001	25.64[1]		138.85	0.14	b.d.l.				b.d.l.	2.69	b.d.l.	b.d.l.	b.d.l.	b.d.l.	b.d.l.		b.d.l.	0.94	5.02		b.d.l.	b.d.l.		0.03	0.24		b.d.l.																b.d.l.
BR16	29/10/2017	136.29	0.02	1543.94	0.22	b.d.l.	b.d.l.	b.d.l.	0.02	0.06	b.d.l.	0.01	b.d.l.	0.05	b.d.l.	b.d.l.	b.d.l.	0.06	2.94	1.93	b.d.l.		b.d.l.	b.d.l.	0.21	0.04	b.d.l.	0.00	b.d.l.	0.03	b.d.l.	b.d.l.	b.d.l.	b.d.l.	b.d.l.	b.d.l.	b.d.l.	b.d.l.	b.d.l.	b.d.l.	b.d.l.	b.d.l.	b.d.l.	0.00
BR16	30/07/2016	101.86	0.03	1048.57	0.19	b.d.l.	b.d.l.	b.d.l.	0.02	0.05	0.02	b.d.l.	b.d.l.	0.08	0.00	0.01	b.d.l.		2.45	6.52	b.d.l.		b.d.l.	b.d.l.	0.18	0.26	b.d.l.	0.00	b.d.l.	b.d.l.	b.d.l.	b.d.l.	b.d.l.	b.d.l.	b.d.l.	b.d.l.	b.d.l.	b.d.l.	b.d.l.	b.d.l.	b.d.l.	b.d.l.	b.d.l.	0.00
BR21	23/08/2016	4.62	0.02	13.41	0.04	b.d.l.	b.d.l.	b.d.l.	0.01	0.03	12.72	b.d.l.	0.00	0.00	0.00	0.02	b.d.l.		0.17	15.33	0.00		b.d.l.	b.d.l.	0.01	0.72	b.d.l.	0.00	b.d.l.	b.d.l.	b.d.l.	b.d.l.	b.d.l.	0.02	b.d.l.	b.d.l.	b.d.l.	b.d.l.	b.d.l.	b.d.l.	b.d.l.	b.d.l.	b.d.l.	0.00
DUP	15/06/2015	0.77	0.00	1.82	0.01	b.d.l.	b.d.l.			b.d.l.	3.22	0.00	0.00	0.03	b.d.l.	b.d.l.		0.00	0.15	3.96		b.d.l.	0.00			0.11		b.d.l.																
EDN	16/05/2015	1.73	b.d.l.	1.85	b.d.l.	0.03	b.d.l.			b.d.l.	3.04	0.08	0.01	0.61	b.d.l.	b.d.l.		b.d.l.	0.07	8.71		b.d.l.	b.d.l.			0.07		b.d.l.																
GDS	17/06/2015	0.58	b.d.l.	0.62	0.01	0.03	b.d.l.			b.d.l.	0.01	b.d.l.	b.d.l.	0.15	0.01	0.01		0.00	0.13	10.89		b.d.l.	0.00			0.01		b.d.l.																
GDS	Sanjuan et al., 2001	0.58[1]		2.04	0.01	b.d.l.				b.d.l.	b.d.l.	b.d.l.	b.d.l.	0.19	b.d.l.	b.d.l.		b.d.l.	0.16	11.18		b.d.l.	b.d.l.		b.d.l.	b.d.l.		b.d.l.																b.d.l.
IRN	05/05/2017	1.35	b.d.l.	7.86	b.d.l.	b.d.l.	b.d.l.	b.d.l.	0.02	0.06	1.06	b.d.l.	0.03	0.53	0.00	0.01	b.d.l.	0.01	0.56	1.01	b.d.l.		b.d.l.	b.d.l.	0.00	0.00	b.d.l.	b.d.l.	b.d.l.	b.d.l.	b.d.l.	b.d.l.	b.d.l.	b.d.l.	b.d.l.	b.d.l.	b.d.l.	b.d.l.	b.d.l.	b.d.l.	b.d.l.	b.d.l.	b.d.l.	b.d.l.
IRN	15/06/2017	1.33	b.d.l.	8.14	b.d.l.	b.d.l.	b.d.l.	b.d.l.	0.01	0.04	b.d.l.	0.00	0.01	0.39	0.01	0.01	b.d.l.	0.00	0.52	0.20	b.d.l.		b.d.l.	b.d.l.	0.00	0.00	b.d.l.	b.d.l.	b.d.l.	0.04	b.d.l.	b.d.l.	b.d.l.	b.d.l.	b.d.l.	b.d.l.	b.d.l.	b.d.l.	b.d.l.	b.d.l.	b.d.l.	b.d.l.	b.d.l.	b.d.l.
IRN	28/07/2017																																											
IRN	30/08/2017	1.34	b.d.l.	9.07	b.d.l.	b.d.l.	b.d.l.	b.d.l.	0.02	0.06	0.02	0.00	0.01	0.34	0.01	0.01	b.d.l.	0.00	0.55	0.12	b.d.l.		b.d.l.	b.d.l.	0.00	0.00	b.d.l.	0.00	b.d.l.	b.d.l.	b.d.l.	b.d.l.	b.d.l.	b.d.l.	b.d.l.	b.d.l.	b.d.l.	b.d.l.	b.d.l.	b.d.l.	b.d.l.	b.d.l.	b.d.l.	b.d.l.
IRN	25/09/2017	1.33	b.d.l.	8.70	b.d.l.	b.d.l.	b.d.l.	b.d.l.	0.02	0.06	b.d.l.	0.00	0.00	0.33	b.d.l.	0.01	b.d.l.	0.00	0.55	0.10	b.d.l.		b.d.l.	b.d.l.	0.00	0.00	b.d.l.	b.d.l.	b.d.l.	b.d.l.	b.d.l.	b.d.l.	b.d.l.	b.d.l.	b.d.l.	b.d.l.	b.d.l.	b.d.l.	b.d.l.	b.d.l.	b.d.l.	b.d.l.	b.d.l.	b.d.l.
IRN	26/10/2017	1.41	b.d.l.	8.23	b.d.l.	b.d.l.	b.d.l.	b.d.l.	0.02	0.06	2.02	0.00	0.03	0.59	0.02	b.d.l.	b.d.l.	0.00	0.55	0.16	b.d.l.		b.d.l.	b.d.l.	0.00	0.00	b.d.l.	b.d.l.	b.d.l.	b.d.l.	b.d.l.	b.d.l.	b.d.l.	b.d.l.	b.d.l.	b.d.l.	b.d.l.	b.d.l.	b.d.l.	b.d.l.	b.d.l.	b.d.l.	b.d.l.	b.d.l.
IRN	29/11/2017	1.28	b.d.l.	8.14	b.d.l.	b.d.l.	b.d.l.	b.d.l.	0.02	0.08	4.59	0.01	0.05	0.71	b.d.l.	0.01	b.d.l.	0.01	0.52	0.08	b.d.l.		b.d.l.	b.d.l.	0.00	0.00	b.d.l.	b.d.l.	b.d.l.	0.02	b.d.l.	b.d.l.	b.d.l.	b.d.l.	b.d.l.	b.d.l.	b.d.l.	b.d.l.	b.d.l.	b.d.l.	b.d.l.	b.d.l.	b.d.l.	b.d.l.
IRN	Sanjuan et	1.44[1]		11.6	b.d.l.	b.d.l.				0.19	8.12	0.16	0.07	1.06	b.d.l.	b.d.l.		b.d.l.	0.60	18.60		b.d.l.	b.d.l.		b.d.l.	0.04		b.d.l.																b.d.l.

Spring	Date	Li (µmol/L)	Be (µmol/L)	B (µmol/L)	F (mmol/L)	Al (µmol/L)	P (mmol/L)	Ti (mmol/L)	V (µmol/L)	Cr (µmol/L)	Mn (µmol/L)	Fe (mmol/L)	Co (µmol/L)	Ni (µmol/L)	Cu (µmol/L)	Zn (µmol/L)	Ga (nmol/L)	As (µmol/L)	Rb (µmol/L)	Sr (µmol/L)	Y (µmol/L)	Ag (µmol/L)	Cd (µmol/L)	In (nmol/L)	Cs (µmol/L)	Ba (µmol/L)	La (nmol/L)	Pb (µmol/L)	Bi (µmol/L)	Ce (nmol/L)	Pr (nmol/L)	Nd (nmol/L)	Sm (nmol/L)	Eu (nmol/L)	Gd (nmol/L)	Tb (nmol/L)	Dy (nmol/L)	Ho (nmol/L)	Er (nmol/L)	Tm (nmol/L)	Yb (nmol/L)	Lu (nmol/L)	Th (µmol/L)	U (µmol/L)
	al., 2001																																											
MAN	16/06/2015	4.09	0.00	4.63	0.01	0.02	0.001			b.d.l.	13.92	0.06	0.02	0.21	b.d.l.	b.d.l.		0.01	0.26	8.33		b.d.l.	b.d.l.			0.15		b.d.l.																
MAN	Sanjuan et al., 2001	4.75[1]		7.9	0.01	b.d.l.				0.10	13.11	0.06	0.03	0.49	b.d.l.	b.d.l.		b.d.l.	0.30	9.13		b.d.l.	b.d.l.		b.d.l.	0.18		b.d.l.															b.d.l.
MAN G	Sanjuan et al., 2001	2.16[1]		4.6	b.d.l.	1.48				b.d.l.	8.85	b.d.l.	0.03	0.41	b.d.l.	b.d.l.		b.d.l.		10.16		b.d.l.	b.d.l.			0.06		b.d.l.															
MANES	15/06/2017				b.d.l.															1.34																						
MANES	Sanjuan et al., 2001	1.01[1]		9.3	b.d.l.	b.d.l.				0.17	9.01	0.13	0.07	1.02	b.d.l.	b.d.l.		b.d.l.	0.47	15.64		b.d.l.	b.d.l.		b.d.l.	b.d.l.		b.d.l.															b.d.l.
OLIV1	Sanjuan et al., 2001	3.17[1]		152.5	0.02	b.d.l.				b.d.l.	0.49	b.d.l.	b.d.l.	b.d.l.	b.d.l.	b.d.l.		b.d.l.		2.62		b.d.l.	b.d.l.			b.d.l.		b.d.l.															
OLIV2	Sanjuan et al., 2001	5.91[1]		1992	0.04	2.97				0.62	5.70	0.01	b.d.l.	0.17	b.d.l.	b.d.l.		b.d.l.	0.82	19.86		b.d.l.	b.d.l.		b.d.l.	0.06		b.d.l.															0.01
PISSA	Sanjuan et al., 2001	0.29[1]		6.8	b.d.l.	b.d.l.				b.d.l.	8.86	0.04	b.d.l.	0.29	b.d.l.	b.d.l.		b.d.l.		28.42		b.d.l.	b.d.l.			b.d.l.		b.d.l.															
RB1	15/10/2016	2.72	0.00	2.59	0.02	b.d.l.	b.d.l.	b.d.l.	0.01	0.02	8.39	0.00	0.07	0.50	0.00	0.01	b.d.l.		0.23	3.90	b.d.l.		b.d.l.	b.d.l.	0.00	0.05	b.d.l.	b.d.l.	b.d.l.	b.d.l.	b.d.l.	b.d.l.	b.d.l.	b.d.l.	b.d.l.	b.d.l.	b.d.l.	b.d.l.	b.d.l.	b.d.l.	b.d.l.	b.d.l.	b.d.l.	0.00
RFOUQ	Sanjuan et al., 2001	0.04[1]		0.0	b.d.l.	b.d.l.				b.d.l.	b.d.l.	b.d.l.	b.d.l.	b.d.l.	b.d.l.	b.d.l.		b.d.l.		7.30		b.d.l.	b.d.l.			b.d.l.		b.d.l.															
RR1	30/07/2016	15.42	0.01	158.93	0.04	b.d.l.	b.d.l.	b.d.l.	0.01	0.03	4.77	b.d.l.	0.01	0.09	b.d.l.	0.02	b.d.l.		0.59	7.21	b.d.l.		b.d.l.	b.d.l.	0.01	0.05	b.d.l.	0.00	b.d.l.	b.d.l.	b.d.l.	b.d.l.	b.d.l.	b.d.l.	b.d.l.	b.d.l.	b.d.l.	b.d.l.	b.d.l.	b.d.l.	b.d.l.	b.d.l.	b.d.l.	0.00
sRMAT	Sanjuan et al., 2001	3.75[1]		7.3	0.01	b.d.l.				b.d.l.	0.42	b.d.l.	b.d.l.	b.d.l.	b.d.l.	b.d.l.		b.d.l.		6.05		b.d.l.	b.d.l.			0.06		b.d.l.															
sRMAT2	Sanjuan et al., 2001	1.58[1]		b.d.l.	b.d.l.	b.d.l.				b.d.l.	0.25	b.d.l.	b.d.l.	0.10	b.d.l.	b.d.l.		b.d.l.		6.51		b.d.l.	b.d.l.			b.d.l.		b.d.l.															
sRMAT3	Sanjuan et al., 2001	0.12[1]		7.0	0.01	1.11				b.d.l.	2.95	0.01	0.05	0.22	0.05	b.d.l.		b.d.l.		8.22		b.d.l.	b.d.l.			0.09		b.d.l.															
TB	22/11/2017	15.85	0.02	196.39	0.12	b.d.l.	b.d.l.	b.d.l.	0.00	0.01	b.d.l.	0.00	b.d.l.	b.d.l.	b.d.l.	0.00	b.d.l.	0.01	0.39	4.82	0.00		b.d.l.	b.d.l.	0.02	0.76	0.03	0.00	b.d.l.	b.d.l.	b.d.l.	0.06	b.d.l.	b.d.l.	b.d.l.	0.01	0.05	b.d.l.	b.d.l.	b.d.l.	b.d.l.	b.d.l.	b.d.l.	0.00
TBA	15/06/2015	1.04	0.00	3.94	0.01	0.04	b.d.l.			b.d.l.	14.14	0.08	0.01	0.11	0.07	0.02		0.00	0.37	9.99		b.d.l.	0.00			0.25		0.00															
TR	21/07/2017	0.89	0.01	1.30	0.03	0.89	b.d.l.	b.d.l.	b.d.l.	b.d.l.	3.39	0.02	b.d.l.	0.01	0.02	0.59	b.d.l.	b.d.l.	0.07	1.85	0.00		b.d.l.	b.d.l.	0.00	0.03	0.70	0.00	b.d.l.	0.94	0.10	0.42	b.d.l.	0.03	0.10	0.04	0.14	0.04	0.07	b.d.l.	0.07	0.01	b.d.l.	b.d.l.
TR	30/01/2018	2.28	0.05	1.76	0.04	1.22	b.d.l.	b.d.l.	b.d.l.	b.d.l.	12.34	0.08	b.d.l.	0.00	0.01	0.16	0.00	b.d.l.	0.11	5.57	0.01		b.d.l.	b.d.l.	0.00	0.06	7.60	0.00	b.d.l.	7.59	0.75	2.81	0.47	0.11	0.58	0.08	0.52	0.12	0.28	0.03	0.14	0.02	b.d.l.	b.d.l.
VERO	15/06/2017				b.d.l.															0.33																						
VERO	30/08/2017				b.d.l.															0.51																						
VERO	Sanjuan et al., 2001	0.86[1]		7.9	b.d.l.	b.d.l.				0.15	7.17	0.11	0.05	0.95	b.d.l.	0.12		b.d.l.	0.54	14.15		b.d.l.	b.d.l.		b.d.l.	b.d.l.		b.d.l.															b.d.l.

[1] Li concentrations on samples from Sanjuan et al (2001) are from this study

Table 3: Carbon species distribution and isotopic ratios in waters and gas in thermal springs of Piton des Neiges. (See Table B.3 for a compilation of data from previous studies).

Spring	pH	Temperature (°C)	TDIC (mM)	H_2CO_3 (mM)	HCO_3 (mM)	$\delta^{13}C_{TDIC}$ (‰ PDB)	$\delta^{13}C_{CO2}$ (‰ PDB)
BACH	6.85	25.6	18.92	4.55	14.38	1.40	
BB	6.7	25.1	26.2	8.10	18.10	-1.39	
BR14	6.8	37.2	32.61	7.86	24.74	-0.78	
BR16	6.5	29.1	38.13	15.39	22.73	0.6	
BR21	6.2	25.1	17.93	10.50	7.43	2.98	
DUP	8.1	23.3	7.36	0.13	7.23	3.40	
EDN	6.41	25.5	43.03	20.03	23.00	3.00	
GDS	7.7	18.7	9.18	0.39	8.79	1.70	
IRN	6.5	35.1	40.35	15.79	24.56	-1.22	
IRN	6.7	35	40.73	11.76	28.97	-0.86	-5.26
IRN	6.4	36.2	38.03	21.73	16.29	-0.78	
IRN	6.4	36	36.16	16.12	20.04	-0.51	-5.39
IRN	6.6	36.2	38.18	12.84	25.33	-0.5	-5.39
IRN	6.4	34.3	37.22	16.70	20.52	-0.36	-5.35
MAN	6.56	30.6	26.84	10.27	16.57	1.60	
MANES	6.4	30.5	40.65	18.56	22.08	-1.43	-5.63
RB1	5.95	19.8	29.30	21.41	7.89	-1.91	
RR1	6.17	32.5	17.77	10.37	7.40	2.61	
TB	6.3	34.4	24.31	12.30	12.01	-1.72	
TR	7.3	20.8	3.53	0.38	3.15	-8.02	
TR	7.5	20.8	4.5	0.31	4.18	-6.36	
VERO	6.2	29.7	37.83	21.68	16.15	-2.16	-5.99
VERO	6.4	29.3	38.48	17.69	20.79	-2.08	-5.79

Temperature, pH and electrical conductivity values at the spring outlets are in the range of 19.2 – 48.0 °C, 5.3 – 7.6, and 312 – 3370 µS/cm, respectively (Table 1). Thermal waters show a mixed composition between Na-Ca-Mg (Figure 2). Most springs are bicarbonate dominated. A few springs, however, show a trend toward the sulfate and/or chloride pole. For instance, the Tuf Rouge spring (TR), is sulfate dominated with sulfate concentrations reaching 765 ppm. The spring of Mafate (MF1) is the only chloride dominated spring. For the majority of springs, the relative proportions of major elements display little variation over time (1 s.d. of Na+K, Ca+Mg, SO_4+Cl, HCO_3 mole fractions ≤ 8%), with the exception of TR that shows larger temporal fluctuations (≤ 18%).

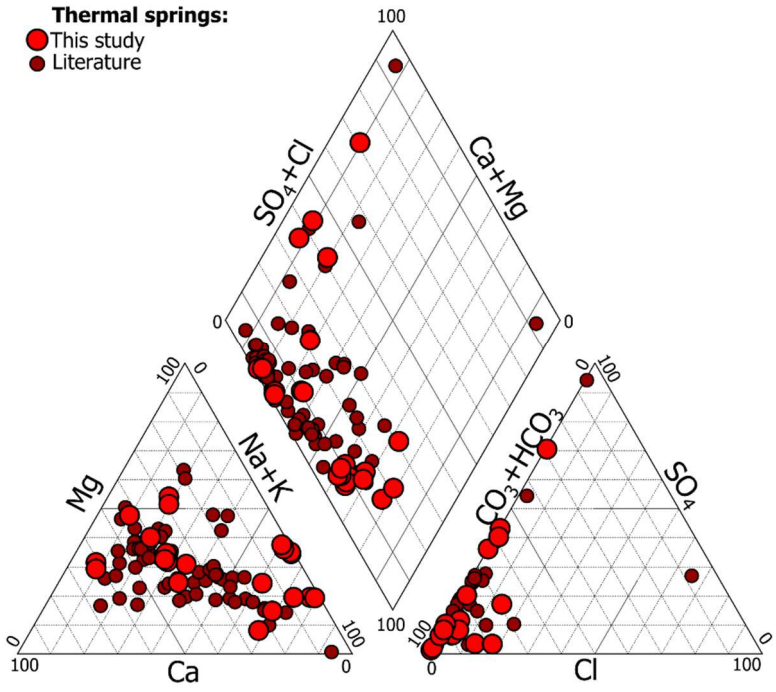

Figure 2: Piper diagram for thermal springs of Piton des Neiges. Literature data are from Belle (2014), Frissant et al. (2003), Iundt et al. (1992), Lopoukhine and Stieltjes (1978), Louvat and Allègre (1997), and Sanjuan et al. (2001). Most springs are bicarbonate dominated.

Total alkalinity (HCO_3) varies from 56 to 2769 ppm. Expressed as TDIC concentrations, springs also analyzed for $\delta^{13}C$ cluster between of 3.5 and 99.2 mM, with two outliers, the MANES spring at 127.8 mmol/L and the OLIV2 spring at 283.7 mmol/L (Table 3). $\delta^{13}C_{TDIC}$ data range from -8.0 to 3.2 ‰, values for the TR spring (-8.0 and -6.4 ‰) being significantly lower than those of other springs. $\delta^{13}C_{CO2}$ values of spring gas range from -6.7 to -5.3 ‰.

$\delta^{18}O_{H2O}$ and δD_{H2O} values for thermal springs range from -8.67 to -4.9 ‰ and from -56.3 to -23.5 ‰ VSMOW, respectively, without any shift from the Local Meteoric Water Line (Table 1, Table B.1, Figure 3). Our new O and D isotopic analyses fall within ± 0.1 ‰ of previous values for the same springs (e.g. IRN, VERO). Importantly, thermal springs are among the most depleted waters in ^{18}O and D of Réunion, their $\delta^{18}O_{H2O}$ and δD_{H2O} values being more negative than those of rivers and groundwater ($-7.1 \leq \delta^{18}O_{H2O} \leq -3.0$ ‰ and $-45.0 \leq \delta D_{H2O} \leq -11.4$ ‰), and only comparable to those of water samples associated with cyclonic events ($-11.8 \leq \delta^{18}O_{H2O} \leq -7.53$ ‰ and $-78.0 \leq \delta D_{H2O} \leq -46.1$ ‰) or to the most depleted rainwater collected at high altitude (≥ 2000 m, $\delta^{18}O_{H2O} = -7.6$ ‰ and $\delta D_{H2O} = -47.0$ ‰, Table C.1).

Major and trace element concentrations are reported in Figure 5 as a function of chloride. In comparison with cold waters, thermal springs are systematically enriched in Na, K, Mg, B, Li and SO_4 for a given Cl concentration (Table 1 andTable 2, Figure 5). Li concentrations of rivers RFER, RBACH and RMAT are respectively 0.01, 0.29 and 0.29 µmol/L.

The $^{87}Sr/^{86}Sr$ ratios of Piton des Neiges thermal springs, reported in Table 1 and Figure 5, fall in a much narrower range (0.704142 to 0.704336) than those of La Réunion cold waters (0.704141 to 0.708227). This narrow range is similar to that of Piton des Neiges rocks (0.704041 to 0.704368), and is much lower than that of seawater offshore Réunion Island (0.709179).

δ^7Li values of most thermal springs range between +7.5 ‰ and +21.8 ‰ (Table 1 and Figure 6), well below seawater (+31 ‰). There are, however, two extreme δ^7Li values in the thermal spring dataset, one at +2 ‰ (BR12) and one at +34.8 ‰ (OLIV2). δ^7Li values of rivers RFER, RBACH and RMAT are respectively of 25.2, 12.1, and 9.7 ‰. The $\delta^{37}Cl$ of thermal springs ranges from the value of seawater (0 ‰) and +0.40 ‰, except for one spring (BR14) showing a negative value of -0.35 ‰ (Table 1 and Figure 6).

5. Discussion

5.1. Origin of water

Major-trace element compositions and isotope analyses are powerful tools to identify the reservoirs supplying the different species in solution, and thus the origin and pathways of hydrothermal fluids in the massif of Piton des Neiges volcano. This identification work must begin with water reservoirs. In a $\delta^{18}O_{H2O}$ vs δD_{H2O} diagram, the plot of Piton des Neiges thermal springs on the local meteoric water line (LMWL) indicates that water is of meteoric origin (Figure 3). As no data significantly depart from the LMWL, it can be inferred that processes such as seawater contamination, evaporation, or exchange with CO_2, H_2S or minerals do not influence largely the O and H isotope composition of thermal springs.

In addition, the strong ^{18}O and D depletion observed in thermal springs compared to other waters may be used to constrain their origin more precisely. Thermal springs have very low $\delta^{18}O_{H2O}$ and δD_{H2O} values compared to rivers, groundwater or to the majority of rainfalls from La Réunion available in the literature (Grunberger, 1989; Nicolini et al., 1991; Aunay and Gourcy, 2007; Aunay et al., 2012; Rogers et al., 2012; Aunay et al., 2013; Petit et al., 2013a, 2013b; Belle, 2014; Gourcy et al., 2018), suggesting a contribution of depleted waters like high altitude rainfalls and cyclones. Indeed, the isotopic signature of rainfalls being strongly controlled by the amount of condensed water (distillation effect), they are usually increasingly depleted in heavy isotopes with increasing altitude as the air masses cool and condensate (Hoefs, 2015). In the existing database for Réunion Island, the highest altitude rainfalls sampled so far outside of a cyclonic event ($\delta^{18}O_{H2O}$ = -7.1 ‰, δD_{H2O} = -41.26 ‰ at 2250 m for the rainy season of 1985-1986) do not reach the depletion of thermal springs (up to -8.67 ‰ and -56.3 ‰ for $\delta^{18}O_{H2O}$ and δD_{H2O}, respectively), and the estimated altitude gradients are not strong enough to explain

their negative $\delta^{18}O_{H2O}$ vs δD_{H2O} signature (Grunberger, 1989; Nicolini et al., 1998, 1991). Nevertheless, it cannot be excluded that high altitude rainfalls yet to be analyzed (for instance close to the Piton des Neiges summit at 3070 m) may control the signature of spring waters. Alternatively, cyclones are another candidate, because those extreme rainfalls represent the most isotopically depleted reservoir of meteoric waters (Lawrence and Gedzelman, 1996). The lowest $\delta^{18}O_{H2O}$, δD_{H2O} values of thermal springs are in the range of those from cyclone waters (Aunay and Gourcy, 2007; Nicolini et al., 1989). In consequence, we interpret thermal spring waters as being supplied largely by cyclones, with a possible contribution from high altitude (≥ 2000 m) rainfalls. From the comparison of our new analyses with available literature data, it seems that the O, H isotope composition of springs is very steady over several decades (e.g. for the IRN spring, Table 1 and supplementary material), and is barely influenced by seasonal variations of rainfall supply. However, the database for rain isotope ratios in La Réunion does not allow us to explore the inter-annual and inter-cyclone variability of isotopes ratios that could fall in the range of the thermal waters (Guilpart et al., 2017). Whatever their origin, this ^{18}O and D depletion indicates that thermal waters do not completely homogenize with cold groundwater, which implies that their pathway is disconnected from the superficial water table.

The absence of ^{18}O enrichment of thermal waters relative to the LMWL also indicates that the isotopic exchange between rocks and water is very limited. As this is well-known, the oxygen isotopic exchange kinetics between water and rocks (mainly silicate and carbonate minerals) is very slow at atmospheric temperature and becomes significant only at high temperature (Panichi and Gonfiantini, 1977). For this reason, ^{18}O enrichment relative to local groundwater is observed for most of the worldwide geothermal waters discharged from high-temperature wells > 180 °C (Panichi and Gonfiantini, 1981). The water/rock ratio may also be an influent parameter on the ^{18}O enrichment of the waters. For example, at similar high temperatures of 300-350 °C, the $\delta^{18}O$ values for the Los Humeros geothermal waters (Mexico, Tello et al., 2000), indicate a much more significant ^{18}O enrichment from the water-rock interactions than that for the Krafla geothermal waters (Iceland, Sveinbjornsdottir et al., 1986), for which the water-rock ratio is higher. In comparison with these geothermal systems, the lack of oxygen isotopic exchange between rocks and thermal waters at Piton des Neiges suggests that their temperatures of interaction are relatively low (< 180 °C) and/or that the water/rock ratios are high enough to buffer the isotopic signature of Réunion basalts (5.5 – 6.6 ‰).

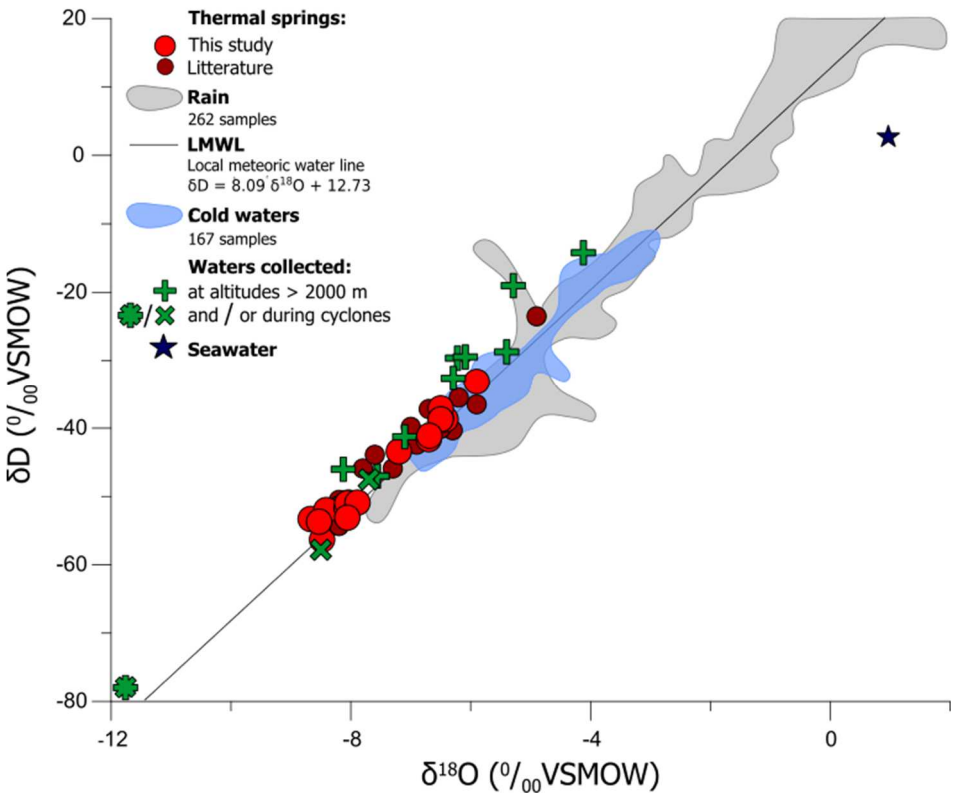

Figure 3: Comparison of $\delta^{18}O_{H2O}$ vs δD_{H2O} values for Piton des Neiges hot springs with rainfalls, cold waters (rivers and groundwater), and seawater from La Réunion. Datasets for rainwater and cold waters (grey and blue shaded contours, respectively) do not include waters collected at altitudes > 2000 m and waters associated with cyclonic events. These two subsets, detailed in Table C.1, are represented separately: cyclone waters (tilted green crosses), waters collected at altitudes > 2000 m (straight green crosses), cyclone waters collected at altitudes > 2000 m (combined tilted and straight green crosses). The local meteoric water line is the linear regression for the total rainwater dataset. Thermal springs plot on the meteoric water line. Some thermal springs show a strong depletion in ^{18}O and D compared to low-altitude rainfalls and cold waters. Literature data are from Grunberger (1989), Nicolini et al. (1991), Sanjuan et al. (2001), Frissant et al. (2005), Aunay and Gourcy (2007), Aunay et al. (2012), Rogers et al. (2012), Aunay et al. (2013), Petit et al. (2013a; 2013b), Belle (2014), and Gourcy et al. (2018).

5.2. Origin of carbon

Because CO_2 bubbling is observed at the outlet of several springs (e.g. IRN, BC), the original composition of thermal waters prior to degassing must be reconstructed for interpreting TDIC and $\delta^{13}C$ data. Following the equations detailed in Ruzié et al. (2013), we thus estimated the initial (pre-degassing) TDIC and $\delta^{13}C_{TDIC}$ as a function of the the final TDIC, $\delta^{13}C_{TDIC}$, $\delta^{13}C_{CO2}$, temperature, and pH using an open system Rayleigh distillation law. As CO_2 degassing fractionates ^{12}C into the gas phase and ^{13}C into the liquid phase, the initial $\delta^{13}C_{TDIC}$ of the solution is bracketed between the final values of $\delta^{13}C_{TDIC}$ (-4.5 to 3.4 ‰) and $\delta^{13}C_{CO2}$ (-6 to -5.3 ‰). For the majority of thermal springs, the initial fluid that best fits the observed compositions and carbon isotopic signatures has thus a $\delta^{13}C_{TDIC}$ of -5 ‰, a pH of 5.4, and a TDIC of 200 to 400 mmol/L (Figure 4a). This initial fluid is inferred to degas at a temperature of 50 to 100 °C, and a P_{CO2} of 0.9 to 3 MPa. Our pre-degassing $\delta^{13}C_{TDIC}$ value of -5 ‰ is consistent with a mantle

carbon signature (Deines, 2002). It is also in agreement with the $\delta^{13}C_{CO2}$ of fumaroles (-4.1 ‰, Marty et al., 1993) and the $\delta^{13}C$ of xenolith fluid inclusions (-4.6 to -3.7 ‰ (Trull et al., 1993), at Piton de la Fournaise.

Two $\delta^{13}C_{TDIC}$ data belonging to the TR spring (-8 and -6.4 ‰) are too low to come from the Rayleigh distillation of a solution at -5 ‰. These low values are possibly explained by a biogenic end-member contribution ($\delta^{13}C_{CO2} \leq$ -20 ‰) or by re-dissolution of degassed and fractionated magmatic CO_2 (Liuzzo et al., 2015). Alternatively, it is possible that magmatic degassing processes might also fractionate exsolved carbon (Boudoire et al., 2018). Two other springs, MANES and OLIV2, have too high TDIC values to explain their $\delta^{13}C_{TDIC}$ by Rayleigh distillation from the above initial solution. These abnormal values may either correspond to an extremely high initial TDIC (≥ 1 mol/L), or to an incorrect measurement of the pH at the outlet. The second interpretation is favored in the case of MANES, showing a surprisingly low pH value for this analysis (5.33) compared to anterior and posterior pH measurements (6 to 6.6) of the same spring. For all the other springs, we conclude that the origin of dissolved carbon is essentially magmatic, a conclusion also reached by Marty et al. (1993).

Studies of secondary minerals at Piton des Neiges report the occurrence of abundant hydrothermal calcite precipitation in the porosity of basalts (Famin et al., 2016; Rançon, 1985), deposited by past episodes of magmatic carbon degassing. Such calcite may represent a significant carbon pool with a magmatic $\delta^{13}C$ signature. This raises the question as to whether the dissolved magmatic carbon found in springs is supplied by a re-dissolution of secondary calcite, or by an actively degassing magma. In a HCO_3 vs (Ca + Mg) diagram, the majority of springs plot above the carbonate dissolution line, even in presence of extra CO_2 (Figure 4b). Calcite dissolution alone is thus unable to explain the HCO_3 enrichment. This leaves primary degassing of an active magma as the largest source of TDIC.

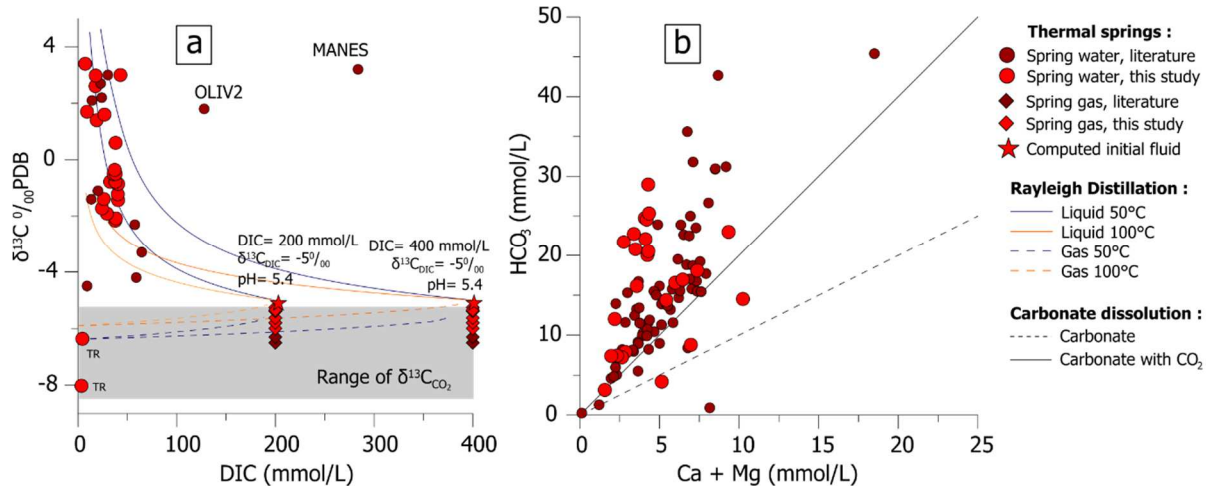

Figure 4: (a) $\delta^{13}C_{TDIC}$ (‰ PDB) versus Dissolved Inorganic Carbon (mM) for water and gas in thermal springs of Piton des Neiges, La Réunion. Degassing lines are represented for two possible initial fluid concentrations and for

different temperatures. Error bars are shorter than symbols. (b) HCO_3 versus Ca+Mg molar concentrations for thermal springs of Piton des Neiges, with equilibrium lines for carbonate (calcite) dissolution with and without carbon dioxide. Thermal springs are enriched in HCO_3^- compared to calcite dissolution lines. Literature data are from (Aunay et al., 2013; Frissant et al., 2003; Iundt et al., 1992; Lopoukhine and Stieltjes, 1978; Louvat and Allègre, 1997; Marty et al., 1993; Sanjuan et al., 2001).

5.3. Origin of mineralization

Major and trace elements

The absence of NO_3^- in springs, and their location at altitudes usually higher than inhabited or farmed lands, indicate that there is no significant anthropogenic contribution to this mineralization. Given the magmatic origin of carbon, other species dissolved in hydrothermal waters may be supplied by degassing magmas. Additionally or alternatively, dissolved species may come from seawater mixing or water-rock interaction such as rock leaching or dissolution of fossil fumarolic deposits. Seawater mixing and water-rock interaction may be explored using diagrams of species concentration vs [Cl] (Figure 5). In such diagrams, dissolved species concentrations barely show any correlation with [Cl] below a threshold of ~0.2 mmol/L Cl, and plot on the line of basalt compositions. This suggests that for springs having low Cl concentrations (hereafter labelled "Group 1"), leaching of basaltic rocks is the main source of mineralization (Figure 5a-b). Spring outlets provide a lower bound of ~50 °C for the temperature of water-rock interaction. Above 0.2 mmol/L Cl (Group 2), most species depart from a simple rock leaching line. For instance, some springs display Na/Cl or K/Cl ratios compatible with a small contamination (≤ 3 mol%) of rock-leaching waters by seawater (Group 2a, Figure 5 c-g). However, other springs have too elevated F, B, Li, Cs, and Rb concentrations at a given [Cl] to be explained by mixing of rock-leaching waters with seawater. The high F/Cl, B/Cl, Li/Cl, Cs/Cl, and Rb/Cl ratios in these springs (Group 2b) require an additional source for these elements, such as selective mineral dissolution or magmatic degassing. We note that Cl, F, B, Li, Cs and Rb are volatile elements in magmas from Piton de la Fournaise undergoing low-pressure differentiation and degassing (Vlastélic et al., 2011). This analogy pleads in favor of a dissolution of gas or fumarolic deposits from a differentiated melt within Piton des Neiges. Given the lack of correlation between TDIC and Cl, F, B, Li, Cs or Rb concentrations, the source of these species is independent from the carbon source.

Table 4: Classification of thermal springs of Piton des Neiges in three groups according to mineralization processes, and their associated geochemical profiles in major trace elements, $\delta^{7}Li$ and $\delta^{37}Cl$ values.

	Group 1	**Group 2a**	**Group 2b**
Thermal springs	AGS, BACH, BC, BE, BR1, BR10, BR11, BR12, BR13, BR15, BR18, BR2, BR27, BR3, BR4, BR5, BR6, BR7, BR8, BR9, DUP, EDN, FJ1, FJ2, FJ3, G1, G2, G3, G4, GDS, IRN, MAN, MAN G, MANES, OLIVbis, PC, PISSA, RB1, RFOUQ, sRMAT, sRMAT2, TBA, TR, VERO	BB, MF1, OLIV2, sRMAT3	BR12, BR14, BR16, BR17, BR21, IMA, OLIV1, RR1, TB
$\delta^{18}O$ and δD	-8.67 to -4.9 ‰ VSMOW and 56.3 to -23.5 ‰ VSMOW Meteoric water, mostly cyclone and/or high altitude rains		
$\delta^{13}C$	-8.0 to 3.2 ‰ PDB Mostly magmatic CO_2		
Major and trace elements	Cl<0.2 mmol/L and enrichment in other elements along basalt composition	Cl>0.2 mmol/L and enrichment in other elements by seawater mixing	Cl>0.2 mmol/L and enrichment in Na, F, B, Li, Cs, Rb above seawater mixing
$^{87}Sr/^{86}Sr$	0.704142 to 0.704336 Interaction with Reunion Island rocks		
$\delta^{7}Li$	+7.5 to +16.6 ‰ LSVEC Interaction with basalt	+18 to +34.8 ‰ LSVEC Mixing with seawater	+2 ‰ LSVEC Interaction with differentiated magma or their gas products/condensates
$\delta^{37}Cl$	No data	+0.06 to +0.35 ‰ SMOC Mixing with seawater	-0.35 to +0.4 ‰ SMOC Mixing with seawater and magmatic input
$\delta^{34}S$	+2.0 to +5.8 ‰ CDT Magmatic sulfur	+3.0 to +8.9 ‰ CDT Magmatic sulfur with seawater mixing	+4.8 ‰ CDT Mostly magmatic sulfur
Spatial repartition	In Sill zones, rift zone N30°E and inside the proposed caldera rim	Outside the proposed caldera rim	Near syenite intrusions

Strontium isotopes

Our classification of Piton des Neiges thermal springs into three groups, summarized in Table 4, may be compared with isotope data which provide additional information about the relative contribution of each pool to the mineralization of spring waters. Among them, the $^{87}Sr/^{86}Sr$ ratio is a good tracer of water-rock interaction or seawater contamination. The narrow range of $^{87}Sr/^{86}Sr$ values obtained for spring waters (0.704142 to 0.704336), irrespective of Cl concentration and consistent with Piton des Neiges volcanic rocks (0.704041 to 0.704368), clearly indicates that strontium concentration is buffered by water-rock interaction in all the thermal springs of Groups 1 and 2 (Figure 5h). This $^{87}Sr/^{86}Sr$ signature contrasts with that of cold waters, increasingly influenced by seawater (0.709179) at increasing [Cl] (Figure 5h). It is thus manifest that seawater contamination is too limited to affect the Sr isotopic signature of thermal springs, no matter their group.

Lithium isotopes

The δ^7Li signature of waters is used as a tracer of hydrothermal alteration and water-rock interaction. At Piton des Neiges, the lowest lithium concentration is found in a surface water from the Ferrière river in Cilaos (RFER), whose δ^7Li of +25.2 ‰ is interpreted as reflecting the isotopic signature of rain water. Group 1 thermal springs display decreasing δ^7Li values from +16.6 to +7.5 ‰ with increasing lithium concentration (Figure 6a; Table 4). Given the δ^7Li range of Réunion basalts (+3.9 to +4.4 ‰, Krienitz et al., 2012), this decreasing trend suggests, in agreement with element analyses (Figure 5), that Group 1 springs results from meteoric water interaction with basaltic rocks, as documented in pore waters leaching basalts from Iceland, Hawaii or the Columbia River (Liu et al., 2015, 2013; Pogge von Strandmann et al., 2012; Ryu et al., 2014). The two samples from Salazie rivers (RBACH and RMAT) mimic the decreasing trend at lower [Li], probably because these streams collect springs belonging to Group 1.

Lithium isotopes are also convenient to identify contamination by seawater due to its high δ^7Li (+31 ‰), or by magmatic inputs due to their negative δ^7Li (≤ -1.3 ‰ at Piton de la Fournaise (Vlastélic et al., 2011). At increasing lithium concentration, Group 2a springs (BB, sRMAT3 and OLIV2) show an increasing δ^7Li trend (up to +34.8 ‰) with increasing [Li]. As for Na vs Cl or K vs Cl diagrams (Figure 5 a-b), we interpret this increasing δ^7Li trend as an influence of seawater in Group 2a, the most contaminated spring being OLIV2 (Table 4). Group 2b springs (OLIV1, BR12) fall at the high [Li], low δ^7Li end of the meteoric water / rock interaction trend, with BR12 showing the lowest δ^7Li value of our dataset (+2 ‰). This low value cannot be accounted for by water interaction basalt because it is below the range of available data for La Réunion basalts (+3.9 and 4.4 ‰). At Piton de la Fournaise, Vlastélic et al. (2011) have shown that degassing-induced Li fractionation during magma differentiation could produce very light lithium compositions in fumarolic deposits (-2.8 ≤ δ^7Li ≤ -1.3 ‰), and even lighter lithium compositions in differentiated (trachytic) melts (-21 ≤ δ^7Li ≤ -17 ‰). As for element ratios in Group 2 springs (Figure 5c-g), we conclude that the low δ^7Li signature of BR12 is thus either compatible with leaching of a very differentiated rock, or with the incorporation of depleted lithium from magmatic gas or fumarolic deposits.

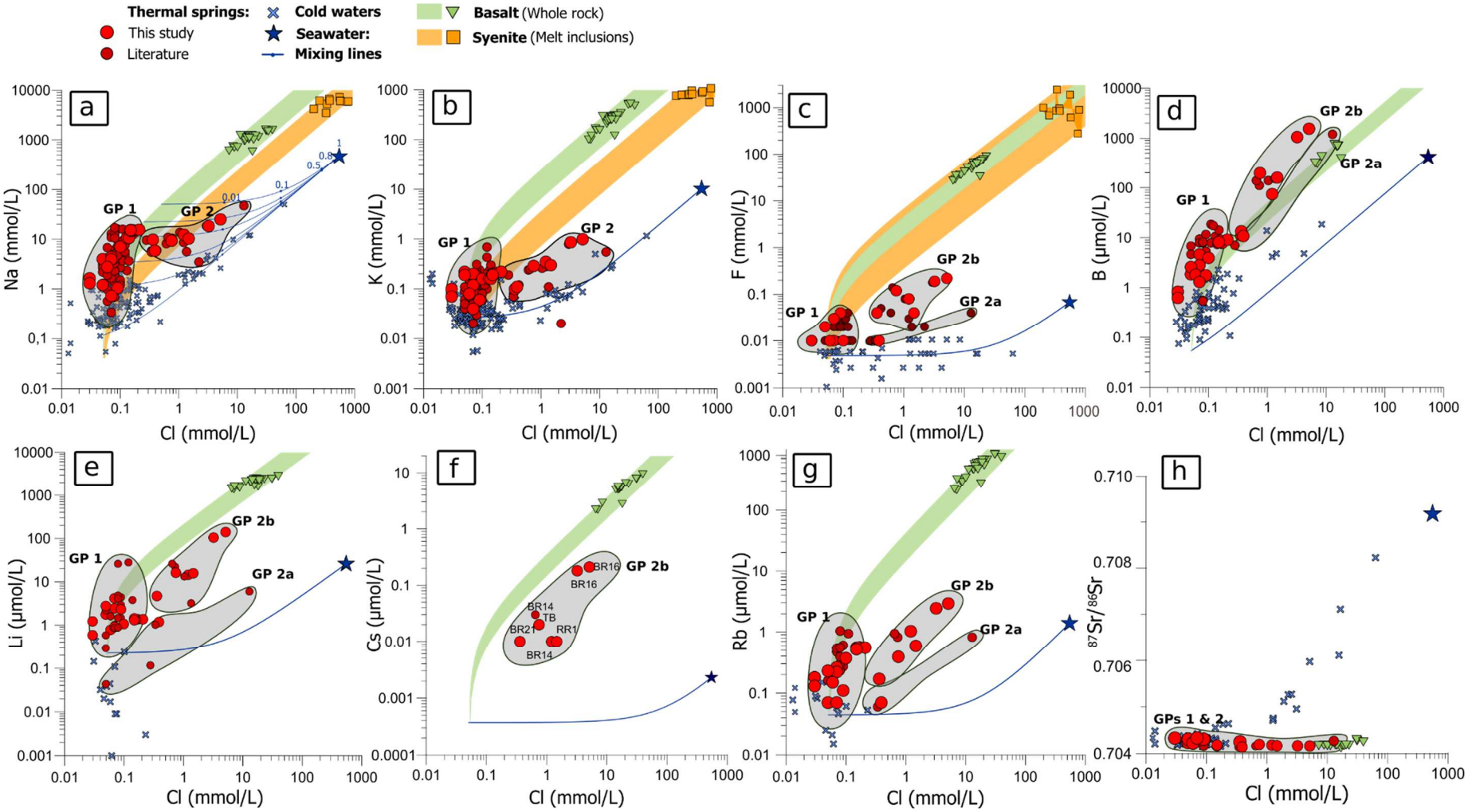

Figure 5: Comparison of Na, K, F, B, Li, Cs, Rb, $^{87}Sr/^{86}Sr$ vs Cl molar concentrations for Piton des Neiges thermal springs with cold waters (rivers and groundwater), seawater and mafic and differentiated rocks (basalt whole rock and melt inclusions from syenite, respectively) from Réunion. Literature data are from (Aunay et al., 2013, 2012; Aunay and Gourcy, 2007; Belle, 2014; Frissant et al., 2005, 2003; Iundt et al., 1992; Lopoukhine and Stieltjes, 1978; Louvat and Allègre, 1997; Nauret et al., 2019; Petit et al., 2013a, 2013b; Rogers et al., 2012; Sanjuan et al., 2001; Smietana, 2011; Vigouroux et al., 2009; Vlastélic et al., 2013, 2007, 2005; Welsch et al., 2013)). Thermal springs can be subdivided into three groups according to their chemical composition. Error bars are shorter than symbols.

Chlorine isotopes

$\delta^{37}Cl$ represents a promising geochemical tool under development to track the origin of Cl in hydrothermal fluids. Because of the ~10 mg/L analytical limit, all the springs analyzed for $\delta^{37}Cl$ belong to Group 2. Both Groups 2a and 2b show a clear mixing trend of decreasing $\delta^{37}Cl$ from +0.4 ‰ at low Cl concentration, to seawater at 0 ‰ at high Cl concentration, except for BR14 from Group 2b that stands out with a negative $\delta^{37}Cl$ value of -0.4 ‰ (Figure 6b). To compare these data with the still limited database of worldwide chlorine isotope analyses, we chose those coming from the same laboratory in order to avoid inter-laboratory comparisons. In this even more restricted dataset, tropical ocean island rainwater fall in the range of -0.17 to 0.38 ‰, whereas mantle magmas and arc magmas are thought to display rather negative average $\delta^{37}Cl$ values (-3.0 to -0.2 ‰, see Li et al., (2015) for a review and discussion). In consequence, we interpret the +0.4 ‰ $\delta^{37}Cl$ signature of low-chlorinity springs, such as BR21 (Group 2b), as reflecting the signal of rainwater. As in other spaces, OLIV2 (Group 2a), the most Cl enriched spring of La Réunion, is also the one showing the greatest $\delta^{37}Cl$ influence of seawater (at 0 ‰) with a $\delta^{37}Cl$ of 0.06 ‰. As shown by other tracers, the negative $\delta^{37}Cl$ of spring BR14 in Group 2b (-0.4 ‰) is consistent with a magmatic origin. The two data for spring BR16 (also Group 2b) suggest that the wet season drags Cl concentration and $\delta^{37}Cl$ toward lower values, perhaps because the water recharge flushes seawater downward in the island, thus enhancing the contribution of magmatic Cl. The spring OLIV1 (Group 2a) might also be influenced by this magmatic input. From these data, we infer that Cl is mostly of marine origin for all the springs of Group 2, with a small magmatic contribution essentially apparent in Group 2b (Table 4).

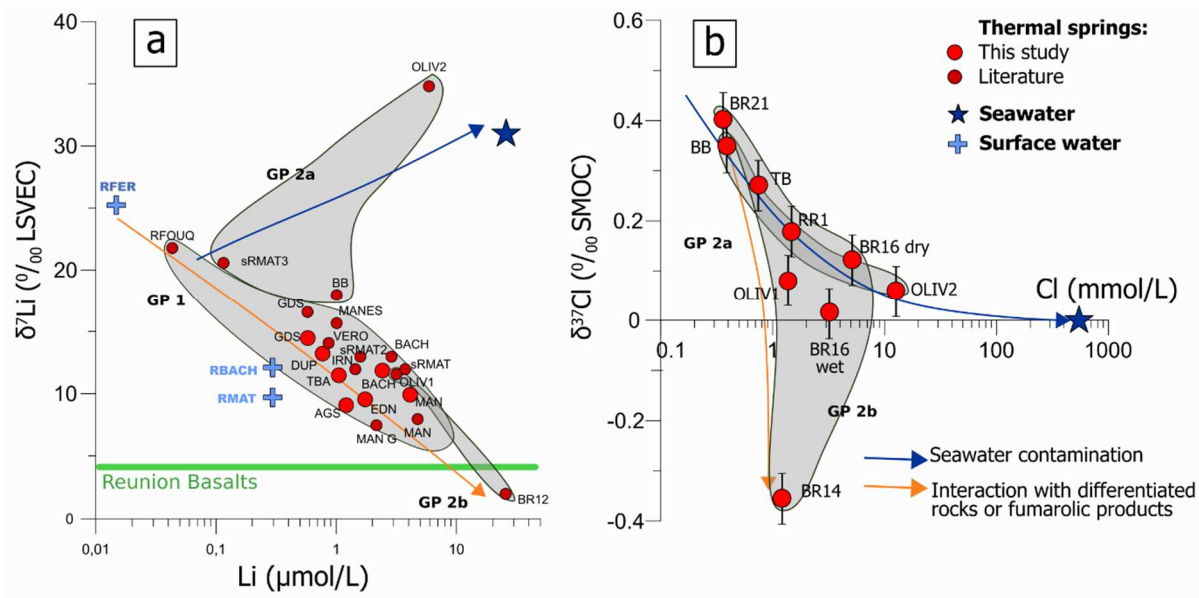

Figure 6: (a) $\delta^{7}Li$ vs Li concentration, and (b) $\delta^{37}Cl$ vs Cl concentration for waters of Piton des Neiges. $\delta^{7}Li$ and $\delta^{37}Cl$ show two trends, one toward seawater, the other one toward dissolution of a very differentiated rock, of magmatic gas or of fumarolic deposits. $\delta^{7}Li$ error bars are shorter than symbols.

491 *Sulfur isotopes*

492 Literature sulfur isotopes data bring further support to our interpretation of seawater and
493 fumarolic inputs in Piton des Neiges hydrothermal system (Table 4). Indeed, (Sanjuan et al.,
494 2001) report nine $\delta^{34}S_{SO4}$ analyses of thermal springs enriched in sulfates. One of them, the
495 spring OLIV2 belonging to Group 2a, displays a high $\delta^{34}S_{SO4}$ at +8.9 ‰, consistent with a slight
496 contamination of this spring by SO_4 from seawater (at $\delta^{34}S_{SO4}$=20 ‰). The eight other springs,
497 belonging to Groups 1 and 2, have $\delta^{34}S_{SO4}$ values between +2.0 and +5.8 ‰, consistent with
498 the signature of SO_4 degassed from a basaltic melt (+2 ‰). In the study area, there is evidence
499 of fossil and active fumarolic sulfide deposits (Lopoukhine and Stieltjes, 1978; Rançon and
500 Rocher, 1985). Like other volatile species, dissolved SO_4 may thus come from the dissolution of
501 magmatic gas or from the oxidation of magmatic sulfur condensates.

502 *Spatial repartition*

503 Most of the thermal springs (Groups 1 and 2) and other hydrothermal indicators are located at
504 the intersection of two or three of the preferential magma intrusion zones (the N030-040 and
505 N120-160 rift zones and/or a sill zone), suggesting that the junctions of these intrusion zones are
506 more favorable to geothermal activity (Figure 7). However, the majority of thermal springs also
507 occur within the perimeter of the proposed caldera associated with the terminal stage of Piton
508 des Neiges activity. It is thus not possible to determine which structure is the primary pathway
509 for geothermal fluid circulation. Nevertheless, two other important features of spatial repartition
510 become apparent when thermal springs are plotted according to our group subdivision (Table 4):
511 (1) Group 2a springs are restricted to the outer rim of the hydrothermal system, outside the
512 proposed caldera of the terminal volcanic stage, and (2) Group 2b are located in the vicinity of
513 the major syenite intrusions interpreted as delineating the caldera. The first observation suggests
514 that the proposed caldera, if it does exist, acts as a hydrological barrier isolating the inner part of
515 the hydrothermal system from seawater contamination. The second observation designates
516 syenite dykes as possible candidates responsible for the interaction of Group 2b springs with
517 highly differentiated rocks or magmatic gas.

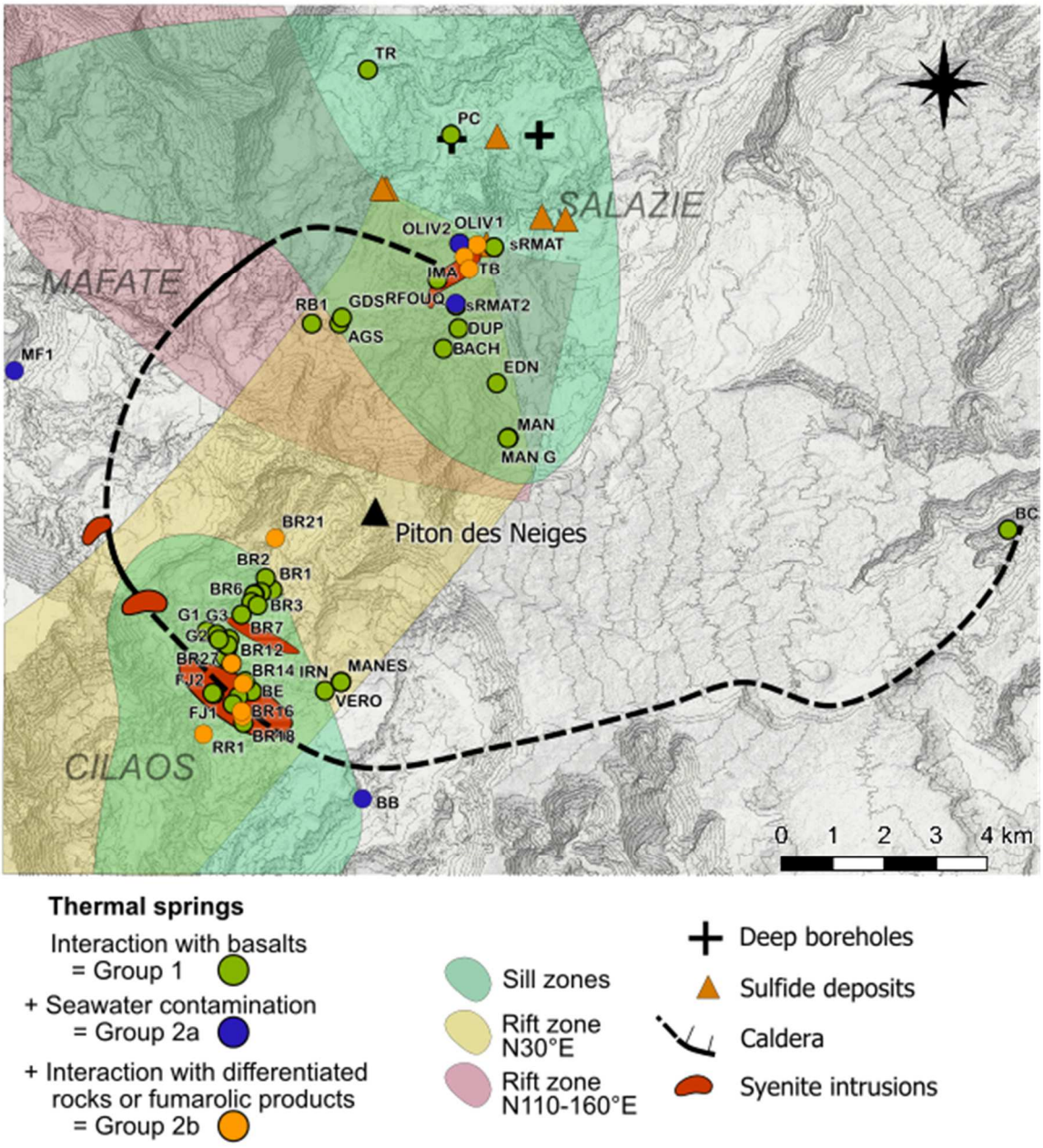

Figure 7: Map of the thermal springs of Piton des Neiges, classified in three groups according to mineralization processes from their geochemical profiles in major trace elements, $\delta^{7}Li$ and $\delta^{37}Cl$ values. Map in UTM coordinates (EPSG:2975, RGR92 / UTM 40s, relief contours at 100 m intervals) from RGE ALTI® - IGN.

5.4. Architecture of hydrothermal circulation

Our new chemical analyses, combined with literature data, may be used to bring constraints on the geometry of Piton des Neiges' hydrothermal system, as illustrated in Figure 8. A first important constraint is that water, carbon and other dissolved species are provided by independent pools. Cyclones or heavy rains and/or high altitude rainfalls that penetrate into the volcanic edifice are the main contributors to the recharge of the thermal aquifer. Carbon is of

primary magmatic origin and dissolves in the thermal aquifer. Three independent pools contribute to the other species dissolved in thermal waters: 1) interaction with basalt at temperature ≥50 °C for all the springs (Groups 1 and 2 springs) enhanced by dissolved CO_2, 2) slight seawater contamination on the outer rim of the hydrothermal system, possibly delimited by a caldera (Group 2a), and/or 3) interaction with a differentiated rock such as syenite, or dissolution of magmatic gas or fumarolic deposits (Group 2b).

Where is the magma at the origin of carbon discharge in hydrothermal waters located? The solubility of carbon in silicate melts is very low compared to other volatile species (e.g. H_2O, S, Cl,). This solubility decreases with decreasing pressure, and thus with the ascent of magmas. Starting from a mantle carbon composition, a rising basaltic melt loses about 80% of its CO_2 before entering the Réunion edifice at ~7 km depth (Di Muro et al., 2016). The source of magmatic carbon can thus be located at any depth from the base of the island to the upper mantle. In Réunion Island, seismic crises at 10 – 20 km depth have been correlated with spikes of soil carbon fluxes and concentration at the surface (Boudoire et al., 2017). This suggests that carbon degassing and ascent occurs at the scale of the whole island, from a magmatic source located in the oceanic crust or in the mantle. Thermal springs have also a mantle helium isotopic signature (Marty et al., 1993; Trull et al., 1993). Therefore, it is more probable that the TDIC of thermal waters is supplied by deep regional degassing of the Réunion hot spot rather than by a shallow magma within Piton des Neiges volcano. Carbon is mixed with thermal waters during its ascent toward the surface.

On the other hand, elements like S, Cl, F, and perhaps B, Li, Rb, and Cs are much more soluble volatile species than CO_2 in silicate melts, and degas at low pressure in the case of basaltic liquids (0 – 200 MPa). The source of these volatile or semi-volatile elements in Group 2b springs is either a degassing magma or an accumulation of fossil condensates deposited by former degassing. It is located at shallow depth within the volcanic edifice (0 – 7 km depth), and is independent from the carbon supply.

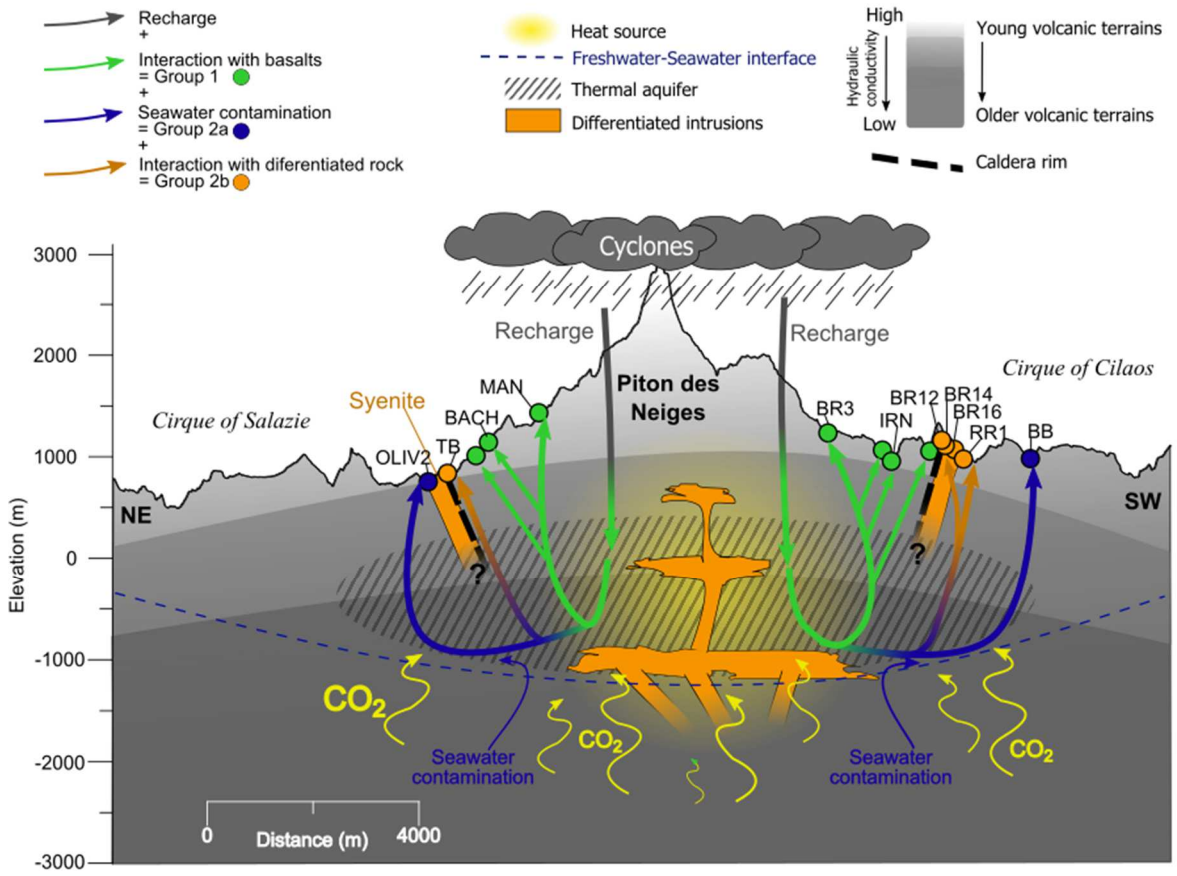

Figure 8: Conceptual model of Piton des Neiges' hydrothermal system. Meteoric water from cyclones and heavy rains penetrates in the edifice and is heated by intrusions of the terminal activity of the volcano. Magmatic CO_2 from regional extent degassing mixes with thermal water and increases its acidity. Temperature and acidity enhance water-rock interaction with the basaltic edifice, as recorded in all the springs. Group 1 springs are entirely mineralized by this process. Group 2 springs show an additional source of mineralization by slight seawater contamination (< 3 mol%). Seawater contamination is most apparent in springs from the outer parts of the hydrothermal system (Group 2a), possibly delimited by a caldera. A few springs, located near syenite intrusions associated with the terminal activity of the volcano, are also mineralized by interaction with a differentiated rock (like the syenite) or with volatiles exsolved from a differentiated magma.

The heat source of the hydrothermal system is neither the source of carbon nor of other volatile elements, because springs interact with rocks no matter their concentration in C, S, Cl, F, B, Li, Rb, and Cs. This inference has to be put in parallel with the low contamination of the hydrothermal system by seawater, only found as a low contribution (<3 mol%, Group 2a) in the lowermost and outermost springs of Piton des Neiges. By comparison, seawater is the dominant water source in most hydrothermal systems from other ocean island volcanoes such as Pantelleria, Azores and Guadeloupe (Carvalho et al., 2006; Gianelli and Grassi, 2001; Sanjuan et al., 1999). Even in geothermal systems alimented by meteoric such as Krafla in Iceland and Maui in Hawaii (Arnórsson, 1995a; Thomas, 1984), Cl enrichment is seldom as low as for the Group 1 thermal springs of Piton des Neiges (Fig. 9). The hydrothermal system of Piton des Neiges is thus exceptionally isolated from seawater compared with the above examples. This exceptional isolation may be explained by the conjunction of several factors. First, the hydrothermal system,

as viewed from thermal springs, is likely protected from seawater by hydrological barriers such as intrusions, faults, or low-permeability layers. In particular, structural studies emphasize the abundance of sills at Piton des Neiges (Chaput et al., 2017, 2014), which may prevent any vertical transport of seawater. The spatial repartition of Group 2 springs suggests that the syenite dykes and/or the terminal caldera of the volcano may also act as hydrological barriers isolating the hydrothermal system. In addition, pore clogging by minerals of the phrenite-pumpellyite facies occurs in all the units older than 640 ka that constitute the basement of Piton des Neiges (Chevalier, 1979; Chovelon, 1968; Famin et al., 2016; Join et al., 2016). However, secondary mineral precipitation also occurs in Hawaii and the Azores (Cruz, 2003; Izquierdo, 2014; Schiffman et al., 2006) and thus hardly explains alone the isolation of the hydrothermal system from seawater in our case. Another hypothesis is that the strong input of meteoric water increases the hydraulic head in the center of the massif, thus lowering the freshwater/seawater interface and flushing seawater outward and downward. Réunion Island has higher precipitation rates than Pantelleria, Iceland or the Azores, but not than Hawaii or Guadeloupe, which calls for an additional factor. At Piton de la Fournaise, in many respects considered as an active analogue of Piton des Neiges, the uppermost magma reservoir feeding most of the eruption is located at 0 to +500 m (Peltier et al., 2008). Following this analogy, we suggest the hydrothermal system of Piton des Neiges is isolated from seawater because its heat source is located at or above sea level, in conjunction with being protected by low permeability barriers and an intense supply of freshwater under tropical climate.

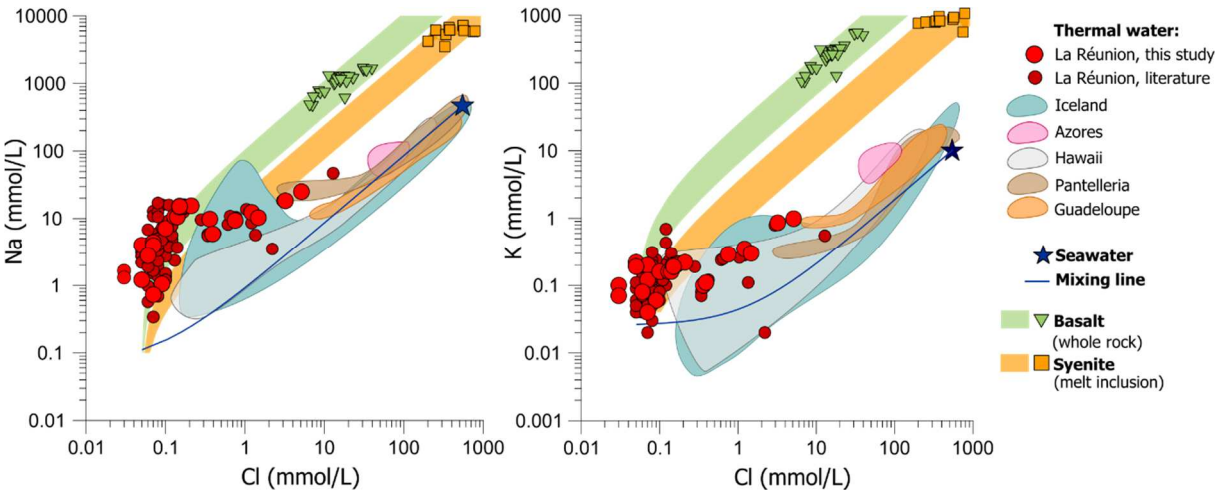

Figure 9: Comparison of Na and K vs Cl molar concentrations for Piton des Neiges thermal springs with thermal water from Iceland, Azores, Hawaii, Pantelleria, Guadeloupe, and with seawater and rocks from Réunion. Literature data are from Arnórsson (1995a, 1995b), Belle (2014), Boivin and Bachèlery (2009), Carvalho et al. (2006), Fretzdorff and Haase (2002), Frissant et al. (2003), Gianelli and Grassi (2001), Iundt et al. (1992), Lopoukhine and Stieltjes (1978), Louvat and Allègre (1997), Sanjuan et al. (2001, 1999), Smietana (2011), Thomas (1984), Vigouroux et al. (2009), Vlastélic et al. (2013, 2007, 2005), Welsch et al. (2013). Compared to other geothermal systems in oceanic islands, the hydrothermal system of Piton des Neiges is exceptionally disconnected from seawater.

608 Our preferred model of hydrothermal circulation has implications for the future of geothermal
609 prospection at Piton des Neiges. In particular, the isolation of thermal waters from seawater is a
610 promising clue that the heat source may be reached by drilling depths of ~1000 m (i.e. sea
611 level), if boreholes are implanted in the cirques at +1000 m. This drilling depth is similar to that
612 of maximum temperature in Pantelleria (Fulignati et al., 1997) and twice less than the depth of
613 the Krafla geothermal field in Iceland (Arnórsson, 1995a). On the other hand, this isolation also
614 implies that production might be limited by the meteoric recharge. In this respect, time series of
615 stable isotopes analyses will be necessary to determine if thermal springs fluctuate in tandem
616 with cyclonic precipitation (i.e. small aquifer) or are steady in time (aquifer large enough to be
617 buffered by long-term recharge). Our study also shows that thermal waters interact with
618 differentiated rocks and/or with volatiles or fumarolic deposits degassed from shallow
619 differentiated magmas. Again, this situation is very similar to that of Pantelleria, for which the
620 hydrothermal system is related to syenite intrusions in the vicinity of caldera faults. Future
621 prospection should thus focus on the spatial repartition of differentiated intrusions and hot
622 springs, taking into account their chemistry to identify pathways of preferential circulation. The
623 occurrence of volatiles species degassed from shallow magmas in springs also questions the age
624 of the last intrusive activity of Piton des Neiges, which might be considerably younger than its
625 terminal eruption at 12, 22 or 29 ka.

626 **6. Conclusion**

627 By combining major/trace element chemistry with a large number of isotopic tools (O, H, C,
628 Sr, Li, Cl), our study untangles the complex history of fluid mixing from multiple pools at the
629 origin of Piton des Neiges' hydrothermal system. Water is of meteoric origin, principally supplied
630 by cyclones and/or high altitude precipitation, with no significant contribution from either rivers
631 or cold groundwater. Unlike in many ocean island volcanoes, seawater does not participate in the
632 recharge feeding the thermal springs, except as a slight contaminant at the external rim of the
633 hydrothermal system. Thermal water is mixed with magmatic carbon, probably originating from
634 regional mantle degassing, and interacts with basaltic rocks at temperatures ≥50 °C. The
635 absence of ^{18}O enrichment of the thermal waters relative to local groundwaters indicates that
636 their oxygen isotope exchange with rocks is limited, and therefore suggests that their
637 temperatures of interaction are relatively low (<180 °C) and/or that waters buffer the oxygen
638 isotope composition of rocks. Higher-than-seawater B/Cl, F/Cl, Cs/Cl, Li/Cl and Rb/Cl ratios as
639 well as low Li and Cl isotopic ratios suggest that some thermal waters also dissolve magmatic
640 gases or fumarolic deposits exsolved from shallow (intra-edifice) differentiated trachytic melts.
641 Whether this input corresponds to an active magma reservoir or to fossil evaporites remains
642 uncertain.

643 Our study provides insights on the architecture of the hydrothermal system of key importance
644 for future geothermal exploration. Thermal waters are protected from shallow aquifers by low-
645 porosity barriers, and their recharge occurs mostly during exceptional rain events. The
646 noteworthy lack of seawater in the hydrothermal system, exceptional for this kind of geological
647 environments, implies that convection cells are located above the seawater/freshwater interface.
648 The heat source, of trachytic nature and disconnected from the magmatic carbon source, may
649 thus be reached within reasonable drilling depths (≤ 1000 m). These results may serve as a basis
650 to design the next step of geothermal exploration, oriented toward estimating the maximum
651 temperature of the deep geothermal waters (using solute chemical and isotope geothermometers
652 integrated into a multicomponent modelling approach) and the size of the hydrothermal
653 reservoir.

654 ## 7. Acknowledgments

655 We thank Jonas Greve and Victor K/Bidi for their participation in the fieldwork and the
656 Établissement thermal de Cilaos for giving us access to their facilities and resources. The Ph.D.
657 fellowship of B. Bénard is funded by Le Conseil Régional de La Réunion. We thank also B. Minster
658 for her help in the analysis of water isotope ratios. The δ^7Li analyses from 2001 were performed
659 by R. Millot (BRGM) within the framework of the ADEME-BRGM project GHEDOM. This research
660 has been supported by INSU-CNRS and OSU-Réunion grants, by EDENA, and by IPGP
661 multidisciplinary program PARI and Paris–IdF region SESAME (Grant no. 12015908). This is IPGP
662 contribution XXXX

663 ## 8. References

664 Adams, M.C., 1996. Chemistry of fluids from ascension #1, a deep geothermal well on ascension
665 island, South Atlantic Ocean. Geothermics, Geothermal Exploration on Ascension Island
666 25, 561–579. https://doi.org/10.1016/0375-6505(96)00011-9
667 Arnórsson, S., 1995a. Geothermal systems in Iceland: Structure and conceptual models—I. High-
668 temperature areas. Geothermics 24, 561–602. https://doi.org/10.1016/0375-
669 6505(95)00025-9
670 Arnórsson, S., 1995b. Geothermal systems in Iceland: Structure and conceptual models—II. Low-
671 temperature areas. Geothermics 24, 603–629. https://doi.org/10.1016/0375-
672 6505(95)00026-7
673 Assayag, N., Rivé, K., Ader, M., Jézéquel, D., Agrinier, P., 2006. Improved method for isotopic
674 and quantitative analysis of dissolved inorganic carbon in natural water samples. Rapid
675 Commun. Mass Spectrom. 20, 2243–2251. https://doi.org/10.1002/rcm.2585
676 Aunay, B., Dewandel, B., Ladouche, B., Oliva, Z., Saussol, P., 2012. Identification des modalités
677 d'exploitation des ressources en eaux souterraines du domaine d'altitude de l'Est de La
678 Réunion – Phase 3 (secteur des Plaines) (No. RP-59245-FR
679 http://infoterre.brgm.fr/rapports/RP-59245-FR.pdf). BRGM.
680 Aunay, B., Gourcy, L., 2007. Approche hydrogéochimique pour la détermination de l'origine de la
681 contamination des eaux. (No. RP-55535-FR http://infoterre.brgm.fr/rapports//RP-55535-
682 FR.pdf). BRGM.

683 Aunay, B., Lucas, C., Ladouche, B., Vigouroux, P., Belle, P., 2013. Identification du potentiel en
684 eau minérale gazeuse du cirque de Salazie (No. RC-62181-FR). BRGM.
685 Belle, P., 2014. Contribution des processus hydrologiques et hydrogéologiques aux glissements
686 de terrain de grande ampleur. Application au contexte tropical de La Réunion. Université
687 de La Réunion, Saint-Denis, La Réunion.
688 Bertani, R., 2005. World geothermal power generation in the period 2001–2005. Geothermics 34,
689 651–690. https://doi.org/10.1016/j.geothermics.2005.09.005
690 Boivin, P., Bachèlery, P., 2009. Petrology of 1977 to 1998 eruptions of Piton de la Fournaise, La
691 Réunion Island. J. Volcanol. Geotherm. Res., Recent advances on the geodynamics of
692 Piton de la Fournaise volcano 184, 109–125.
693 https://doi.org/10.1016/j.jvolgeores.2009.01.012
694 Bonifacie, M., Monnin, C., Jendrzejewski, N., Agrinier, P., Javoy, M., 2007. Chlorine stable
695 isotopic composition of basement fluids of the eastern flank of the Juan de Fuca Ridge
696 (ODP Leg 168). Earth Planet. Sci. Lett. 260, 10–22.
697 https://doi.org/10.1016/j.epsl.2007.05.011
698 Boudoire, G., Liuzzo, M., Di Muro, A., Ferrazzini, V., Michon, L., Grassa, F., Derrien, A.,
699 Villeneuve, N., Bourdeu, A., Brunet, C., Giudice, G., Gurrieri, S., 2017. Investigating the
700 deepest part of a volcano plumbing system: Evidence for an active magma path below
701 the western flank of Piton de la Fournaise (La Réunion Island). J. Volcanol. Geotherm.
702 Res. 341, 193–207. https://doi.org/10.1016/j.jvolgeores.2017.05.026
703 Boudoire, G., Rizzo, A.L., Di Muro, A., Grassa, F., Liuzzo, M., 2018. Extensive CO 2 degassing in
704 the upper mantle beneath oceanic basaltic volcanoes: First insights from Piton de la
705 Fournaise volcano (La Réunion Island). Geochim. Cosmochim. Acta 235, 376–401.
706 https://doi.org/10.1016/j.gca.2018.06.004
707 Carvalho, M.R., Forjaz, V.H., Almeida, C., 2006. Chemical composition of deep hydrothermal
708 fluids in the Ribeira Grande geothermal field (São Miguel, Azores). J. Volcanol. Geotherm.
709 Res. 156, 116–134. https://doi.org/10.1016/j.jvolgeores.2006.03.015
710 Chaput, M., Famin, V., Michon, L., 2017. Sheet intrusions and deformation of Piton des Neiges,
711 and their implication for the volcano-tectonics of La Réunion. Tectonophysics 717, 531–
712 546. https://doi.org/10.1016/j.tecto.2017.08.039
713 Chaput, M., Pinel, V., Famin, V., Michon, L., Froger, J.-L., 2014. Cointrusive shear displacement
714 by sill intrusion in a detachment: A numerical approach. Geophys Res Lett 41 1937–1943.
715 Chevalier, L., 1979. Structures et évolution du volcan Piton des Neiges. Ile de la Réunion. Leurs
716 relations avec les structures du bassin des Mascareignes. Océan indien occidental
717 (Thèse). Université scientifique et médicale de Grenoble.
718 Chovelon, P., 1968. Forage géothermique de Salazie (SLZ1). Étude géologique du forage et
719 dossier des ouvrages exécutés. (No. N°86CFG018).
720 Cruz, J.V., 2003. Groundwater and volcanoes: examples from the Azores archipelago. Environ.
721 Geol. 44, 343–355. https://doi.org/10.1007/s00254-003-0769-2
722 Deines, P., 2002. The carbon isotope geochemistry of mantle xenoliths. Earth-Sci. Rev. 58, 247–
723 278. https://doi.org/10.1016/S0012-8252(02)00064-8
724 Delibrias, G., Guillier, M.-T., Labeyrie, J., 1986. Gif Natural Radiocarbon Measurements X.
725 Radiocarbon 28, 9–68. https://doi.org/10.1017/S0033822200060008
726 Deniel, C., Kieffer, G., Lecointre, J., 1992. New 230Th-238U and 14C age determinations from
727 Piton des Neiges volcano, Reunion — A revised chronology for the Differentiated Series.
728 J. Volcanol. Geotherm. Res. 51, 253–267. https://doi.org/10.1016/0377-0273(92)90126-X
729 Dezayes, C., Baltassat, J.M., Famin, V., Bes de Berc, S., 2016. Potential interest areas for the
730 development of geothermal energy in La Reunion Island. Presented at the European
731 Geothermal Congress, Strasbourg, France.
732 Di Muro, A., Métrich, N., Allard, P., Aiuppa, A., Burton, M., Galle, B., Staudacher, T., 2016.
733 Magma Degassing at Piton de la Fournaise Volcano, in: Active Volcanoes of the
734 Southwest Indian Ocean, Active Volcanoes of the World. Springer, Berlin, Heidelberg, pp.
735 203–222. https://doi.org/10.1007/978-3-642-31395-0_12
736 Druecker, M., Fan, P., 1976. Hydrology and Chemistry of Ground Water a in Puna, Hawaiia.
737 Groundwater 14, 328–338. https://doi.org/10.1111/j.1745-6584.1976.tb03123.x

738 Eggenkamp, H.G.M., Middelburg, J.J., Kreulen, R., 1994. Preferential diffusion of 35Cl relative to
739 37Cl in sediments of Kau Bay, Halmahera, Indonesia. Chem. Geol. 116, 317–325.
740 https://doi.org/10.1016/0009-2541(94)90022-1
741 Famin, V., Berthod, C., Michon, L., Eychenne, J., Brothelande, E., Mahabot, M.-M., Chaput, M.,
742 2016. Localization of magma injections, hydrothermal alteration, and deformation in a
743 volcanic detachment (Piton des Neiges, La Réunion). J. Geodyn., Fluids in crustal
744 deformation : fluid flow, fluid-rock interactions, rheology, melting and resources 101,
745 155–169. https://doi.org/10.1016/j.jog.2016.05.007
746 Fretzdorff, S., Haase, K.M., 2002. Geochemistry and petrology of lavas from the submarine flanks
747 of Réunion Island (western Indian Ocean): implications for magma genesis and the
748 mantle source. Mineral. Petrol. 75, 153–184. https://doi.org/10.1007/s007100200022
749 Frissant, N., Gourcy, L., Brach, M., 2005. Recherche d'une relation entre le plateau de Dos-d'Ane
750 et les sources Blanche et Denise (No. RP-54167-FR http://infoterre.brgm.fr/rapports/RP-
751 54167-FR.pdf). BRGM.
752 Frissant, N., Lacquement, F., Rançon, J.P., 2003. Etude du potentiel hydrothermal de la zone
753 amont de la rivière du Bras Rouge (Cirque de Cilaos) -Première phase d'étude- (No. RP-
754 52673-FR http://infoterre.brgm.fr/rapports/RP-52673-FR.pdf). BRGM.
755 Fulignati, P., Malfitano, G., Sbrana, A., 1997. The Pantelleria caldera geothermal system: Data
756 from the hydrothermal minerals. J. Volcanol. Geotherm. Res. 75, 251–270.
757 https://doi.org/10.1016/S0377-0273(96)00066-2
758 Gianelli, G., Grassi, S., 2001. Water–rock interaction in the active geothermal system of
759 Pantelleria, Italy. Chem. Geol. 181, 113–130. https://doi.org/10.1016/S0009-
760 2541(01)00276-5
761 Gillot, P.-Y., Nativel, P., 1982. K-Ar chronology of the ultimate activity of piton des neiges
762 volcano, reunion island, Indian ocean. J. Volcanol. Geotherm. Res. 13, 131–146.
763 https://doi.org/10.1016/0377-0273(82)90024-5
764 Godon, A., Jendrzejewski, N., Eggenkamp, H.G.M., Banks, D.A., Ader, M., Coleman, M.L., Pineau,
765 F., 2004. A cross-calibration of chlorine isotopic measurements and suitability of seawater
766 as the international reference material. Chem. Geol. 207, 1–12.
767 https://doi.org/10.1016/j.chemgeo.2003.11.019
768 Gourcy, L., Renaud, T., Aunay, B., 2018. Etude des modes de transfert et de l'origine des nitrates
769 sur les secteurs de La Saline-l'Hermitage (FRH5) et de Dos d'Ane (Galets Ronds). (No.
770 RP-66338-FR http://infoterre.brgm.fr/rapports//RP-66338-FR.pdf). BRGM.
771 Grunberger, O., 1989. Etude géochimique et isotopique de l'infiltration sous climat tropical
772 contrasté. Massif du Piton des Neiges. Ile de la Réunion (Thèse). Université de Paris XI.
773 Guilpart, E., Vimeux, F., Evan, S., Brioude, J., Metzger, J.-M., Barthe, C., Risi, C., Cattani, O.,
774 2017. The isotopic composition of near-surface water vapor at the Maïdo observatory
775 (Reunion Island, southwestern Indian Ocean) documents the controls of the humidity of
776 the subtropical troposphere. J. Geophys. Res. Atmospheres 122, 9628–9650.
777 https://doi.org/10.1002/2017JD026791
778 Hoefs, J., 2015. Stable Isotope Geochemistry. Springer.
779 Iundt, F., Mauroux, B., Barrera, L., Cruchet, M., Martignoni, P., Stieltjes, L., 1992. Etude des
780 sources thermominérales de Cilaos (No. RR-35833-FR). BRGM.
781 Izquierdo, T., 2014. Conceptual hydrogeological model and aquifer system classification of a
782 small volcanic island (La Gomera; Canary Islands). CATENA 114, 119–128.
783 https://doi.org/10.1016/j.catena.2013.11.006
784 Johnston, J.M., Pellerin, L., Hohmann, G.W., 1992. Evaluation of Electromagnetic Methods for
785 Geothermal Reservoir Detection. Geotherm. Resour. Counc. Trans. 16, 241–245.
786 Join, J.-L., Folio, J.-L., Bourhane, A., Comte, J.-C., 2016. Groundwater Resources on Active
787 Basaltic Volcanoes: Conceptual Models from La Réunion Island and Grande Comore, in:
788 Bachelery, P., Lenat, J.-F., Di Muro, A., Michon, L. (Eds.), Active Volcanoes of the
789 Southwest Indian Ocean. Springer Berlin Heidelberg, Berlin, Heidelberg, pp. 61–70.
790 https://doi.org/10.1007/978-3-642-31395-0_5
791 Join, J.-L., Folio, J.-L., Robineau, B., 2005. Aquifers and groundwater within active shield
792 volcanoes. Evolution of conceptual models in the Piton de la Fournaise volcano. J.

Volcanol. Geotherm. Res. 147, 187–201. https://doi.org/10.1016/j.jvolgeores.2005.03.013
Kluska, J.M., 1997. Evolution magmatique et morpho-structurale du Piton des Neiges au cours des derniers 500000 ans (Thèse). Université de Paris 11, Orsay.
Krienitz, M.-S., Garbe-Schönberg, C.-D., Romer, R.L., Meixner, A., Haase, K.M., Stroncik, N.A., 2012. Lithium Isotope Variations in Ocean Island Basalts—Implications for the Development of Mantle Heterogeneity. J. Petrol. 53, 2333–2347. https://doi.org/10.1093/petrology/egs052
Lawrence, R.J., Gedzelman, D.S., 1996. Low stable isotope ratios of tropical cyclone rains. Geophys. Res. Lett. 23, 527–530. https://doi.org/10.1029/96GL00425
Li, L., Bonifacie, M., Aubaud, C., Crispi, O., Dessert, C., Agrinier, P., 2015. Chlorine isotopes of thermal springs in arc volcanoes for tracing shallow magmatic activity. Earth Planet. Sci. Lett. 413, 101–110. https://doi.org/10.1016/j.epsl.2014.12.044
Liu, X.-M., Rudnick, R.L., McDonough, W.F., Cummings, M.L., 2013. Influence of chemical weathering on the composition of the continental crust: Insights from Li and Nd isotopes in bauxite profiles developed on Columbia River Basalts. Geochim. Cosmochim. Acta 115, 73–91. https://doi.org/10.1016/j.gca.2013.03.043
Liu, X.-M., Wanner, C., Rudnick, R.L., McDonough, W.F., 2015. Processes controlling δ7Li in rivers illuminated by study of streams and groundwaters draining basalts. Earth Planet. Sci. Lett. 409, 212–224. https://doi.org/10.1016/j.epsl.2014.10.032
Liuzzo, M., Di Muro, A., Giudice, G., Michon, L., Ferrazzini, V., Gurrieri, S., 2015. New evidence of CO2 soil degassing anomalies on Piton de la Fournaise volcano and the link with volcano tectonic structures. Geochem. Geophys. Geosystems 16, 4388–4404. https://doi.org/10.1002/2015GC006032
Lopoukhine, M., Stieltjes, L., 1978. Evaluation du Potentiel géothermique de l'Île de la Réunion - 1ère Phase exploratoire : Géologie et géochimie des eaux (No. 78 SGN 467 GTH). BRGM.
Louvat, P., Allègre, C.J., 1997. Present denudation rates on the island of Réunion determined by river geochemistry: Basalt weathering and mass budget between chemical and mechanical erosions. Geochim. Cosmochim. Acta 61, 3645–3669. https://doi.org/10.1016/S0016-7037(97)00180-4
Marty, B., Meynier, V., Nicolini, E., Griesshaber, E., Toutain, J.P., 1993. Geochemistry of gas emanations: A case study of the Réunion Hot Spot, Indian Ocean. Appl. Geochem. 8, 141–152. https://doi.org/10.1016/0883-2927(93)90030-K
McDougall, I., 1971. The geochronology and evolution of the young volcanic island of Réunion, Indian Ocean. Geochim. Cosmochim. Acta 35, 261–288. https://doi.org/10.1016/0016-7037(71)90037-8
Millot, R., Guerrot, C., Vigier, N., 2004. Accurate and High-Precision Measurement of Lithium Isotopes in Two Reference Materials by MC-ICP-MS. Geostand. Geoanalytical Res. 28, 153–159. https://doi.org/10.1111/j.1751-908X.2004.tb01052.x
Nauret, F., Famin, V., Vlastélic, I., Gannoun, A., 2019. A trace of recycled continental crust in the Réunion hotspot. Chem. Geol. 524, 67–76. https://doi.org/10.1016/j.chemgeo.2019.06.009
Nicolini, E., Coudray, J., Grunberger, O., Jusserand, C., 1998. Seasonnal variations in isotopic content (18O-2H) of rainfall over an intertropical humid island (Reunion Island, southwest Indian Ocean). IAHS 253.
Nicolini, E., Jusserand, C., Blavoux, B., Coudray, J., Eberschweiler, C., Mairine, P., Aubouin, J., 1989. Appauvrissement en isotopes lourds des précipitations liées aux cyclones. Comptes Rendues Académie Sci. 309, 1255–1260.
Nicolini, E., Olive, P., Coudray, J., Jusserand, C., 1991. Circulation des eaux dans le massif du Piton de la Fournaise (Ile de la Réunion) et leur contamination par des fluides d'origine magmatique. Comptes Rendues Académie Sci. 312, 535–542.
Panichi, C., Gonfiantini, R., 1981. Geothermal waters. In Stable Isotope Hydrology, Technical Reports Series. INTERNATIONAL ATOMIC ENERGY AGENCY, Vienna.
Panichi, C., Gonfiantini, R., 1977. Environmental isotopes in geothermal studies. Geothermics 6, 143–161. https://doi.org/10.1016/0375-6505(77)90024-4

Peltier, A., Famin, V., Bachèlery, P., Cayol, V., Fukushima, Y., Staudacher, T., 2008. Cyclic magma storages and transfers at Piton de La Fournaise volcano (La Réunion hotspot) inferred from deformation and geochemical data. Earth Planet. Sci. Lett. 270, 180–188. https://doi.org/10.1016/j.epsl.2008.02.042

Petit, V., Aunay, B., Gourcy, L., Baran, N., Oliva, Z., Lucas, C., 2013a. Pollution diffuse et transferts des produits phytosanitaires du sol vers les ressources en eau souterraines de l'île de La Réunion. (No. RP-61477-FR http://infoterre.brgm.fr/rapports//RP-61477-FR.pdf). BRGM.

Petit, V., Dewandel, B., Charlier, J.B., Ollivier, P., Lucas, C., Oliva, Z., 2013b. Amélioration de la connaissance hydrogéologique de l'aquifère côtier du Gol. (No. RP-61834-FR http://infoterre.brgm.fr/rapports//RP-61834-FR.pdf). BRGM.

Pogge von Strandmann, P.A.E., Opfergelt, S., Lai, Y.-J., Sigfússon, B., Gislason, S.R., Burton, K.W., 2012. Lithium, magnesium and silicon isotope behaviour accompanying weathering in a basaltic soil and pore water profile in Iceland. Earth Planet. Sci. Lett. 339–340, 11–23. https://doi.org/10.1016/j.epsl.2012.05.035

Rançon, J.P., 1985. Hydrothermal history of Piton des Neiges volcano (Reunion Island, Indian Ocean). J. Volcanol. Geotherm. Res. 26, 297–315. https://doi.org/10.1016/0377-0273(85)90061-7

Rançon, J.P., Rocher, P., 1985. Découverte de zones fumerolliennes récentes dans le cirque de Salazie (île de La Réunion, Océan Indien). C R Académie Sci. Sér. II 16, 821–826.

Rocher, P., 1988. Contexte volcanique et structural de l'hydrothermalisme récent dans le massif du Piton des neiges (île de La Réunion) : étude détaillée du cirque de Salazie (thesis). Paris 11.

Rogers, K.M., Nicolini, E., Gauthier, V., 2012. Identifying source and formation altitudes of nitrates in drinking water from Réunion Island, France, using a multi-isotopic approach. J. Contam. Hydrol. 138–139, 93–103. https://doi.org/10.1016/j.jconhyd.2012.07.002

Ruzié, L., Aubaud, C., Moreira, M., Agrinier, P., Dessert, C., Gréau, C., Crispi, O., 2013. Carbon and helium isotopes in thermal springs of La Soufrière volcano (Guadeloupe, Lesser Antilles): Implications for volcanological monitoring. Chem. Geol. 359, 70–80. https://doi.org/10.1016/j.chemgeo.2013.09.008

Ryu, J.-S., Vigier, N., Lee, S.-W., Lee, K.-S., Chadwick, O.A., 2014. Variation of lithium isotope geochemistry during basalt weathering and secondary mineral transformations in Hawaii. Geochim. Cosmochim. Acta 145, 103–115. https://doi.org/10.1016/j.gca.2014.08.030

Sanjuan, B., Genter, A., Brach, M., Lebon, D., 2001. Compléments d'étude géothermique dans l'île de la Réunion (géologie, géochimie) (No. RP-51189-FR (http://infoterre.brgm.fr/rapports/RP-51189-FR.pdf)). BRGM.

Sanjuan, B., Lasne, E., Brach, M., Vaute, L., 1999. Bouillante geothermal field (Guadeloupe). Geochemical monitoring during the simulation operation. Critical evaluation of chemical and isotopic field data. (No. RR-40646-FR http://infoterre.brgm.fr/rapports//RR-40646-FR.pdf). BRGM.

Schiffman, P., Watters, R.J., Thompson, N., Walton, A.W., 2006. Hyaloclastites and the slope stability of Hawaiian volcanoes: Insights from the Hawaiian Scientific Drilling Project's 3-km drill core. J. Volcanol. Geotherm. Res., Growth and Collapse of Hawaiian Volcanoes 151, 217–228. https://doi.org/10.1016/j.jvolgeores.2005.07.030

Smietana, M., 2011. Petrology, geochronology (K-Ar) and elemental and isotopic geochemistry (Sr, Nd, Hf, Pb) of older lavas of Reunion : Implications for the construction of the volcanic edifice (Theses). Université de la Réunion.

Sveinbjornsdottir, A.E., Coleman, M.L., Yardley, B.W.D., 1986. Origin and history of hydrothermal fluids of the Reykjanes and Krafla geothermal fields, Iceland. Contrib. Mineral. Petrol. 94, 99–109. https://doi.org/10.1007/BF00371231

Tello, H., Verma, M.P., Tovar, A., 2000. Origin of acidity in the Los Humeros, Mexico, geothermal reservoir, in: Proceedings World Geothermal Congress, Japan. pp. 2959–2966.

Thomas, D.M., 1984. Geothermal resources assessment in Hawaii. Final report (No. DOE/SF/10819-T1). Hawaii Univ., Honolulu (USA). Hawaii Inst. of Geophysics. https://doi.org/10.2172/6761857

903 Trull, T., Nadeau, S., Pineau, F., Polve´, M., Javoy, M., 1993. C-He systematics in hotspot
904 xenoliths: Implications for mantle carbon contents and carbon recycling. Earth Planet. Sci.
905 Lett. 118, 43–64. https://doi.org/10.1016/0012-821X(93)90158-6
906 Vigouroux, N., Williams-Jones, A.E., Wallace, P., Staudacher, T., 2009. The November 2002
907 eruption of Piton de la Fournaise, Réunion: tracking the pre-eruptive thermal evolution of
908 magma using melt inclusions. Bull. Volcanol. 71, 1077. https://doi.org/10.1007/s00445-
909 009-0287-5
910 Violette, S., Ledoux, E., Goblet, P., Carbonnel, J.-P., 1997. Hydrologic and thermal modeling of
911 an active volcano: the Piton de la Fournaise, Reunion. J. Hydrol. 191, 37–63.
912 https://doi.org/10.1016/S0022-1694(96)03071-5
913 Vlastélic, I., Menard, G., Gannoun, A., Piro, J.-L., Staudacher, T., Famin, V., 2013. Magma
914 degassing during the April 2007 collapse of Piton de la Fournaise: The record of semi-
915 volatile trace elements (Li, B, Cu, In, Sn, Cd, Re, Tl, Bi). J. Volcanol. Geotherm. Res. 254,
916 94–107. https://doi.org/10.1016/j.jvolgeores.2012.12.027
917 Vlastélic, I., Peltier, A., Staudacher, T., 2007. Short-term (1998–2006) fluctuations of Pb isotopes
918 at Piton de la Fournaise volcano (Reunion Island): Origins and constraints on the size and
919 shape of the magma reservoir. Chem. Geol. 244, 202–220.
920 https://doi.org/10.1016/j.chemgeo.2007.06.015
921 Vlastélic, I., Staudacher, T., Bachèlery, P., Télouk, P., Neuville, D., Benbakkar, M., 2011. Lithium
922 isotope fractionation during magma degassing: Constraints from silicic differentiates and
923 natural gas condensates from Piton de la Fournaise volcano (Réunion Island). Chem.
924 Geol. https://doi.org/10.1016/j.chemgeo.2011.02.002
925 Vlastélic, I., Staudacher, T., Semet, M., 2005. Rapid Change of Lava Composition from 1998 to
926 2002 at Piton de la Fournaise (Réunion) Inferred from Pb Isotopes and Trace Elements:
927 Evidence for Variable Crustal Contamination. J. Petrol. 46, 79–107.
928 https://doi.org/10.1093/petrology/egh062
929 Welsch, B., Faure, F., Famin, V., Baronnet, A., Bachèlery, P., 2013. Dendritic Crystallization: A
930 Single Process for all the Textures of Olivine in Basalts? J. Petrol. 54, 539–574.
931 https://doi.org/10.1093/petrology/egs077
932

A. Coordinates of the thermal springs

Table A.1: Coordinates of the thermal springs of Piton des Neiges presented in this study.

Spring	X (UTM, RGR92)	Y (UTM, RGR92)	Elevation (m)
AGS	341428	7669771	1234
BACH	343450	7669284	1011
BB	341878	7660557	931
BC	354418	7665780	720
BE	339734	7662634	919
BR1	340133	7664597	1453
BR10	339242	7663434	1008
BR11	339222	7663287	947
BR12	339338	7663175	932
BR13	339601	7662829	906
BR14	339559	7662782	884
BR15	339465	7662529	840
BR16	339529	7662249	791
BR17	339550	7662153	782
BR18	339567	7662024	777
BR2	339999	7664829	1359
BR21	340184	7665618	1661
BR27	339258	7663521	1008
BR3	339912	7664553	1271
BR4	339782	7664516	1185
BR5	339769	7664504	1190
BR6	339721	7664362	1134
BR7	339529	7664121	1078
BR8	339292	7663643	1022
BR9	339260	7663531	1015
DUP	343744	7669677	892
EDN	344487	7668615	1058
FJ1	338996	7662583	1006
FJ2	338966	7662600	1021
FJ3	339358	7662387	928
G1	338855	7663801	1192
G2	339056	7663709	1091
G3	339051	7663737	1101
G4	339090	7663638	1070
GDS	341479	7669885	1197
IMA	343856	7671080	801
IRN	341149	7662647	1117
MAN	344715	7667560	1313
MAN G	344700	7667550	1317
MANECE	341462	7662815	1241
MF1	335119	7668857	885
OLIV1	344106	7671310	681
OLIV2	343763	7671331	777
OLIVbis	343765	7671332	777
PC	343597	7673440	675
PISSA	339842	7664302	1229
RB1	340894	7669768	1335
RFOUQ	343335	7670620	901
RR1	338790	7661807	722
sRMAT	344434	7671264	652
sRMAT2	343700	7670120	841
sRMAT3	343690	7670160	833
TB	343948	7670835	720
TBA	343696	7670129	834
TR	341983	7674700	905
MANECE	341462	7662815	1241

B. Geochemistry of thermal springs: compilation of data from previous studies

Table B.1: Published major elements concentrations, C, O, H, Sr, Li and Cl isotope ratios in thermal springs of Piton des Neiges.

Spring	Campaign	Date	Electrical Conductivity (µS/cm)	pH	Temperature (°C)	Ca (mmol/L)	Mg (mmol/L)	Na (mmol/L)	K (mmol/L)	HCO_3 (mmol/L)	SO_4 (mmol/L)	Cl (mmol/L)	SiO_2 (mmol/L)	CO_3 (mmol/L)	NH_4 (mmol/L)	NO_2 (mmol/L)	NO_3 (mmol/L)	$\delta^{13}C$ (‰ PDB)	$\delta^{18}O$ (‰ VSMOW)	δD (‰ VSMOW)	$^{87}Sr/^{86}Sr$	$\delta^{34}S_{SO4}$ (‰ VCDT)
BACH	Sanjuan et al., 2001	21/10/2000	1540	7.4	19.4	3.6	3.5	5.5	0.2	18.7	0.2	0.1	1.5		b.d.l.	b.d.l.	b.d.l.	-1.1	-6.7	-37.2	0.704300	2.0
BACH	Lopoukhine and Stieltjes, 1978	25/06/1978	1120	7.6	25.6	1.2	3.4	4.8	0.2	15.5	0.2	0.1	1.3		b.d.l.							
BACH	Aunay et al., 2013	12/03/2013	1087	7.0	25.2	2.7	2.4	3.6	0.1	13.9	0.1	0.1	0.4	b.d.l.			b.d.l.					
BB	Sanjuan et al., 2001	24/10/2000	1610	6.7	22.6	4.2	3.4	5.5	0.1	15.4	2.1	0.3	1.9		b.d.l.	b.d.l.	b.d.l.	2.7	-8.2	-54.3	0.704142	3.0
BB	Lopoukhine and Stieltjes, 1978	20/06/1978	1600		26.3	4.0	3.4	5.8	0.1	15.5	2.1	0.3	1.7		b.d.l.							
BC	Lopoukhine and Stieltjes, 1978	06/07/1978		6.5	22.7	4.3	14.2	7.7	0.4	45.4	0.3	0.1	1.8		b.d.l.							
BE	Frissant et al., 2003	01/07/2003	1187	6.3	22.4	3.6	2.1	1.9	0.1	13.2	0.1	0.1	1.6				b.d.l.					
BR1	Frissant et al., 2003	01/07/2003	1364	7.0	17.3	3.4	1.7	6.8	0.1	16.1	0.1	0.1	1.6				b.d.l.					
BR10	Frissant et al., 2003	01/07/2003	950	6.2	18.7	2.1	1.8	1.5	0.0	10.3	0.1	0.1	1.3				b.d.l.					
BR11	Frissant et al., 2003	01/07/2003	896	7.6	20	2.2	1.7	2.0	0.1	9.9	0.1	0.1	1.4				b.d.l.					
BR12	Louvat and Allègre, 1997	1997		6.4	48	1.9	1.7	13.2	0.3	16.7	2.1		2.5									
BR12	Louvat and Allègre, 1997	1997		6.7	47.5	1.5	1.4	12.6	0.3	15.3	1.8	0.1	2.5									
BR12	Lopoukhine and Stieltjes, 1978	20/06/1978	1547	6.7	42	2.0	1.7	10.4	0.3	13.4	1.4	0.7	1.7		b.d.l.							
BR12	Sanjuan et al., 2001	25/10/2000	1430	6.3	36.3	1.6	1.3	10.8	0.3	11.6	2.1	0.6	2.1		b.d.l.	b.d.l.	b.d.l.	2.2	-8.2	-50.5	0.704162	4.8
BR12	Frissant et al., 2003	01/07/2003	1233	6.3	32.6	1.9	1.1	6.0	0.1	8.0	1.6	0.4	1.2				b.d.l.					
BR13	Frissant et al., 2003	01/07/2003	461	7.7	18.1	0.9	1.1	1.0	0.0	4.6	0.1	0.1	0.7				b.d.l.					
BR14	Frissant et al., 2003	01/07/2003	1294	6.8	34.5	2.1	1.5	8.2	0.2	13.2	0.6	0.6	2.0				b.d.l.					
BR15	Frissant et al., 2003	01/07/2003	1100	7.0	19.9	1.9	2.3	2.4	0.2	11.5	0.2	0.1	1.1				0.01					
BR16	Frissant et al., 2003	01/07/2003	2560	6.6	32	2.7	2.1	18.4	0.8	23.9	0.4	3.0	2.1				b.d.l.					
BR17	Frissant et al., 2003	01/07/2003	1262	6.5	27.5	2.1	1.4	8.6	0.3	12.4	1.2	1.2	1.3				b.d.l.					
BR18	Frissant et al., 2003	01/07/2003	656	8.2	23	1.3	0.9	3.0	0.1	6.0	1.0	0.1	0.4				b.d.l.					
BR2	Frissant et al., 2003	01/07/2003	1162	8.1	14.5	2.3	1.3	5.4	0.1	9.1	1.7	0.1	0.7				b.d.l.					
BR27	Iundt et al., 1992	1992	1095	6.6	20.5	1.4	3.4	5.6	0.7	15.0	0.5	0.1	1.0		0.03	b.d.l.	b.d.l.					
BR3	Frissant et al., 2003	01/07/2003	1000	6.3	23.8	3.1	1.3	2.9	0.1	11.9	0.3	0.1	0.7				b.d.l.					
BR4	Frissant et al., 2003	01/07/2003	1156	6.7	16.3	3.3	1.4	1.4	0.1	10.4	0.2	0.1	0.6				b.d.l.					
BR5	Frissant et al., 2003	01/07/2003	1022	7.1	22.2	2.6	1.1	4.8	0.1	11.5	0.2	0.1	1.0				b.d.l.					
BR6	Frissant et al., 2003	01/07/2003	902	6.2	22.1	2.8	0.8	2.7	0.1	8.9	0.5	0.1	0.8				b.d.l.					

Spring	Campaign	Date	Electrical Conductivity (µS/cm)	pH	Temperature (°C)	Ca (mmol/L)	Mg (mmol/L)	Na (mmol/L)	K (mmol/L)	HCO_3 (mmol/L)	SO_4 (mmol/L)	Cl (mmol/L)	SiO_2 (mmol/L)	CO_3 (mmol/L)	NH_4 (mmol/L)	NO_2 (mmol/L)	NO_3 (mmol/L)	$\delta^{13}C$ (‰ PDB)	$\delta^{18}O$ (‰ VSMOW)	δD (‰ VSMOW)	$^{87}Sr/^{86}Sr$	$\delta^{34}S_{SO4}$ (‰ VCDT)
BR7	Frissant et al., 2003	01/07/2003	930	6.3	17.7	3.5	0.9	1.7	0.1	8.2	0.7	0.1	0.9				b.d.l.					
BR8	Frissant et al., 2003	01/07/2003	732	6.9	23.5	2.3	1.1	1.2	0.1	8.0	0.2	0.0	1.1				b.d.l.					
BR9	Frissant et al., 2003	01/07/2003	1003	6.2	26.2	2.4	1.9	2.3	0.1	10.7	0.2	0.1	1.5				b.d.l.					
FJ1	Frissant et al., 2003	30/05/2003	1115	6.8	18.1	2.3	1.9	1.5	0.1	9.9	0.1	0.1	0.9				b.d.l.					
FJ2	Frissant et al., 2003	30/05/2003	1356	6.6	20	3.6	2.6	3.2	0.2	14.7	0.1	0.1	1.5				b.d.l.					
FJ3	Frissant et al., 2003	30/05/2003	479	6.5	19.6	1.1	1.1	0.3	0.0	4.8	0.1	0.1	0.7				b.d.l.					
G1	Frissant et al., 2003	29/05/2003	1370	6.9	16.8	3.5	1.8	5.0	0.2	14.4	0.3	0.1	1.2				b.d.l.					
G2	Frissant et al., 2003	29/05/2003	1312	6.9	15	2.8	2.6	2.7	0.1	13.8	0.1	0.1	1.7				b.d.l.					
G3	Frissant et al., 2003	29/05/2003	1296	6.6	20.2	3.1	2.4	2.3	0.1	13.6	0.1	0.1	1.8				b.d.l.					
G4	Frissant et al., 2003	29/05/2003	1405	6.2	21.6	3.1	2.4	3.7	0.2	13.7	0.1	0.1	1.8				b.d.l.					
GDS	Sanjuan et al., 2001	26/10/2000		6.6	18.6	4.6	2.2	1.3	0.1	8.4	2.9	0.1	0.7		b.d.l.	b.d.l.	b.d.l.	-1.4	-4.9	-23.5	0.704336	3.6
GDS	Aunay et al., 2013	09/11/2011	1086	6.6	19.5	3.0	2.0	1.3	0.1	9.0	1.5	0.1	0.3	b.d.l.			b.d.l.					
IMA	Lopoukhine and Stieltjes, 1978	20/06/1978	1864	6.7	22.5	2.3	2.0	13.7	0.3	20.1	0.6	1.0	1.1		b.d.l.							
IRN	Sanjuan et al., 2001	24/10/2000	2370	6.0	37.8	4.6	4.6	16.1	0.2	31.2	1.1	0.1	2.6		b.d.l.	b.d.l.	b.d.l.		-8.2	-51.3	0.704169	5.3
IRN	Louvat and Allègre, 1997	1997		6.5	37.7	4.3	4.2	15.4	0.2	30.9	1.2		2.4									
IRN	Louvat and Allègre, 1997	1997		6.3	37.5	3.0	4.1	17.0	0.2	31.8	0.6	0.1	2.2									
IRN	Lopoukhine and Stieltjes, 1978	20/06/1978	2733	6.1	38.5	4.3	4.2	15.9	0.2	31.0	0.9	0.1	2.3		b.d.l.							
IRN	Iundt et al., 1992	1992	1953	6.0	36.9	3.2	3.7	14.4	0.2	25.0	1.1	0.2	2.5		b.d.l.	b.d.l.	b.d.l.					
MAN	Sanjuan et al., 2001	19/10/2000	1580	6.6	30.6	4.1	3.4	5.0	0.2	19.2	0.1	0.1	2.0		b.d.l.	b.d.l.	b.d.l.	3	-7.6	-43.9	0.704282	5.6
MAN	Louvat and Allègre, 1997	1997		6.6	30.2	3.2	2.6	4.0	0.2	15.8	0.0	0.1	1.6									
MAN	Lopoukhine and Stieltjes, 1978	24/06/1978	1601	6.2	30.5	3.5	3.2	5.3	0.2	35.6	0.1	0.1	1.8		b.d.l.							
MAN	Belle, 2014	01/12/2011	1596	6.4	31.4	3.6	3.1	4.9	0.2	18.8	0.1	0.1	2.0	b.d.l.			b.d.l.		-7.3	-45.9	0.704287	
MAN	Aunay et al., 2013	06/03/2012	1369	6.2	31.3	3.2	2.8	4.3	0.2	16.6	0.1	0.1	1.7	b.d.l.			0.02		-6.9	-42.4	0.704277	
MAN G	Sanjuan et al., 2001	19/10/2000	1333	7.9	19	4.0	3.0	2.7	0.1	15.8	0.1	0.0	1.6		b.d.l.	b.d.l.	b.d.l.		-7.0	-39.8		
MANES	Sanjuan et al., 2001	24/10/2000	2260	5.3	31	4.0	4.1	12.9	0.2	26.7	0.8	0.1	2.1		b.d.l.	b.d.l.	b.d.l.	3.2	-8.2	-54.3		
MANES	Iundt et al., 1992	1992	1632	6.0	30.1	3.4	3.5	11.4	0.2	22.5	0.7	0.1	2.1		b.d.l.	b.d.l.	b.d.l.					
MF1	Lopoukhine and Stieltjes, 1978	29/06/1978	483	9.4	16	0.1	0.0	3.5	0.0	0.3	0.4	2.2	0.9	0.17	b.d.l.							
OLIV1	Sanjuan et al., 2001	01/10/2000	994	7.3	18.9	1.4	1.3	5.7	0.1	8.2	0.5	1.4	0.7		b.d.l.	b.d.l.	b.d.l.	-4.5	-6.5	-40.1		3.0
OLIV2	Sanjuan et al., 2001	26/10/2000	4980	6.1	26	4.1	4.6	47.0	0.5	42.7	3.2	12.9	0.8		b.d.l.	b.d.l.	b.d.l.	1.8	-7.8	-45.9	0.704270	8.9
OLIVbis	Aunay et al., 2013	12/02/2013	765	7.6	18.6	2.3	1.4	1.8	0.1	5.5	1.7	0.1	0.3	b.d.l.			0.01					
PC	Aunay et al., 2013	03/09/2012	478	7.3	21.6	1.2	1.1	0.6	0.2	5.0	0.1	0.1	0.8	b.d.l.			0.01					
PISSA	Sanjuan et al., 2001	26/10/2000	1190	6.7	18.4	4.4	1.4	3.1	0.0	11.6	1.3	0.0	1.3		b.d.l.	b.d.l.	b.d.l.		-6.7	-41.4		

Spring	Campaign	Date	Electrical Conductivity (µS/cm)	pH	Temperature (°C)	Ca (mmol/L)	Mg (mmol/L)	Na (mmol/L)	K (mmol/L)	HCO_3 (mmol/L)	SO_4 (mmol/L)	Cl (mmol/L)	SiO_2 (mmol/L)	CO_3 (mmol/L)	NH_4 (mmol/L)	NO_2 (mmol/L)	NO_3 (mmol/L)	$\delta^{13}C$ (‰ PDB)	$\delta^{18}O$ (‰ VSMOW)	δD (‰ VSMOW)	$^{87}Sr/^{86}Sr$	$\delta^{34}S_{SO4}$ (‰ VCDT)
RFOUQ	Sanjuan et al., 2001	01/10/2000	1000	7.4	19.2	2.9	2.3	2.2	0.0	11.3	0.3	0.0	0.7		b.d.l.	b.d.l.	b.d.l.		-6.5	-37.9		
RFOUQ	Lopoukhine and Stieltjes, 1978	25/06/1978	1418	6.1	22.5	4.1	3.3	3.3	0.1	16.8	0.4	0.1	1.5		b.d.l.							
sRMAT	Sanjuan et al., 2001	01/10/2000		7.9	18	1.9	6.0	3.7	0.3	17.7	0.5	0.1	1.2		b.d.l.	b.d.l.	b.d.l.		-5.9	-36.5		
sRMAT2	Sanjuan et al., 2001	21/08/2000	716	7.1	21.2	1.9	1.4	1.9	0.1	8.2	0.1	0.1	0.5		b.d.l.	b.d.l.	b.d.l.		-6.2	-35.5		
sRMAT3	Sanjuan et al., 2001	01/10/2000	1380	7.4	26.1	3.5	2.8	9.6	0.2	15.6	2.8	0.3	1.9		0.11	b.d.l.	b.d.l.					
TB	Aunay et al., 2013	01/12/2012	1512	7.0	33.1	1.5	0.7	10.4	0.3	13.9	0.7	0.8	0.9	b.d.l.			b.d.l.					
TBA	Lopoukhine and Stieltjes, 1978	25/06/1978	1752	6.5	27	4.2	2.7	7.2	0.2	17.0	1.8	0.1	1.8		b.d.l.							
TBA	Aunay et al., 2013	12/03/2013	1491	6.8	27.2	4.0	2.3	6.1	0.1	16.1	1.4	0.1	1.4	b.d.l.			b.d.l.					
TR	Belle, 2014	22/11/2011	312	7.1	20.9	0.6	0.6	0.7	0.0	1.3	0.8	0.1	0.5	b.d.l.			b.d.l.					
TR	Aunay et al., 2013	08/03/2012	1453	6.5	21.2	3.7	4.4	1.2	0.1	0.9	8.3	0.1	0.6	b.d.l.			b.d.l.		-6.3	-40.3	0.704310	
VERO	Sanjuan et al., 2001	24/10/2000	2010	5.4	30.3	3.6	3.7	10.9	0.1	23.5	0.7	0.1	2.0		b.d.l.	b.d.l.	b.d.l.		-8.1	-51.2		5.8
VERO	Louvat and Allègre, 1997	1997		6.2	29.6	3.2	3.3	10.4	0.1	22.6	0.7		1.9									
VERO	Louvat and Allègre, 1997	1997		6.2	29.5	3.2	3.2	10.6	0.1	23.9	0.7	0.1	1.9									
VERO	Iundt et al., 1992	1992	1399	6.0	29.2	2.9	3.3	9.4	0.1	19.5	0.6	0.1	1.9		b.d.l.	b.d.l.	b.d.l.					

937

Table B.2: Trace elements concentrations available in the literature for thermal springs of Piton des Neiges.

Spring	Campaign	Date	Li (µmol/L)	Be (µmol/L)	B (µmol/L)	F (mmol/L)	Al (µmol/L)	Cr (µmol/L)	Mn (µmol/L)	Fe (mmol/L)	Co (µmol/L)	Ni (µmol/L)	Cu (µmol/L)	Zn (µmol/L)	As (µmol/L)	Rb (µmol/L)	Sr (µmol/L)	Ag (µmol/L)	Cd (µmol/L)	Cs (µmol/L)	Ba (µmol/L)	Pb (µmol/L)	U (µmol/L)	PO4 (mmol/L)
BACH	Sanjuan et al., 2001	21/10/2000	2.88		5.37	b.d.l.	b.d.l.	b.d.l.	b.d.l.	b.d.l.	b.d.l.	0.12	b.d.l.	b.d.l.	b.d.l.	0.27	10.39	b.d.l.	b.d.l.	b.d.l.	b.d.l.	b.d.l.	b.d.l.	b.d.l.0
BACH	Lopoukhine and Stieltjes, 1978	25/06/1978				b.d.l.				b.d.l.							5.71							
BACH	Aunay et al., 2013	12/03/2013																						
BB	Sanjuan et al., 2001	24/10/2000	1.01		10.64	0.01	b.d.l.	b.d.l.	6.61	0.05	0.05	0.75	b.d.l.	b.d.l.	b.d.l.	0.06	5.48	b.d.l.	b.d.l.	b.d.l.	b.d.l.	b.d.l.	b.d.l.	b.d.l.0
BB	Lopoukhine and Stieltjes, 1978	20/06/1978				0.01				0.08							5.71							
BC	Lopoukhine and Stieltjes, 1978	06/07/1978	27.37			0.04				0.03							2.28							
BE	Frissant et al., 2003	01/07/2003				b.d.l.																		
BR1	Frissant et al., 2003	01/07/2003				0.01																		
BR10	Frissant et al., 2003	01/07/2003				0.01																		
BR11	Frissant et al., 2003	01/07/2003				0.01																		
BR12	Louvat and Allègre, 1997	1997	25.36		181.87											1.12	7.61				0.21			
BR12	Louvat and Allègre, 1997	1997	26.22													1.04	6.09				0.22			
BR12	Lopoukhine and Stieltjes, 1978	20/06/1978	21.61		111.01	0.12				0.01						0.82	7.99							
BR12	Frissant et al., 2003	01/07/2003				0.05																		
BR13	Frissant et al., 2003	01/07/2003				0.01																		
BR14	Sanjuan et al., 2001	25/10/2000	25.64		138.85	0.14	b.d.l.	b.d.l.	2.69	b.d.l.	b.d.l.	b.d.l.	b.d.l.	b.d.l.	b.d.l.	0.94	5.02	b.d.l.	b.d.l.	0.03	0.24	b.d.l.	b.d.l.	b.d.l.0
BR14	Frissant et al., 2003	01/07/2003				0.04																		
BR15	Frissant et al., 2003	01/07/2003				0.01																		
BR16	Frissant et al., 2003	01/07/2003				0.18																		
BR17	Frissant et al., 2003	01/07/2003				0.03																		
BR18	Frissant et al., 2003	01/07/2003				0.01																		
BR2	Frissant et al., 2003	01/07/2003				0.02																		
BR27	Iundt et al., 1992	1992		b.d.l.	17.39	0.02		b.d.l.	7.99	0.04	b.d.l.	b.d.l.	b.d.l.	b.d.l.			4.45	b.d.l.	b.d.l.		b.d.l.			b.d.l.0
BR3	Frissant et al., 2003	01/07/2003				0.02																		
BR4	Frissant et al., 2003	01/07/2003				0.02																		
BR5	Frissant et al., 2003	01/07/2003				0.01																		
BR6	Frissant et al., 2003	01/07/2003				0.02																		
BR7	Frissant et al., 2003	01/07/2003				0.01																		
BR8	Frissant et al., 2003	01/07/2003				0.02																		
BR9	Frissant et al., 2003	01/07/2003				b.d.l.																		
FJ1	Frissant et al., 2003	30/05/2003				0.02																		

Spring	Campaign	Date	Li (µmol/L)	Be (µmol/L)	B (µmol/L)	F (mmol/L)	Al (µmol/L)	Cr (µmol/L)	Mn (µmol/L)	Fe (mmol/L)	Co (µmol/L)	Ni (µmol/L)	Cu (µmol/L)	Zn (µmol/L)	As (µmol/L)	Rb (µmol/L)	Sr (µmol/L)	Ag (µmol/L)	Cd (µmol/L)	Cs (µmol/L)	Ba (µmol/L)	Pb (µmol/L)	U (µmol/L)	PO4 (mmol/L)
FJ2	Frissant et al., 2003	30/05/2003				0.01																		
FJ3	Frissant et al., 2003	30/05/2003				0.02																		
G1	Frissant et al., 2003	29/05/2003				0.01																		
G2	Frissant et al., 2003	29/05/2003				0.03																		
G3	Frissant et al., 2003	29/05/2003				0.03																		
G4	Frissant et al., 2003	29/05/2003				0.03																		
GDS	Sanjuan et al., 2001	26/10/2000	0.58		2.04	0.01	b.d.l.	b.d.l.	b.d.l.	b.d.l.	b.d.l.	0.19	b.d.l.	b.d.l.	b.d.l.	0.16	11.18	b.d.l.	b.d.l.	b.d.l.	b.d.l.	b.d.l.	b.d.l.	b.d.l.0
GDS	Aunay et al., 2013	09/11/2011																						
IMA	Lopoukhine and Stieltjes, 1978	20/06/1978	12.97		138.8	0.08				0.01							7.99							
IRN	Sanjuan et al., 2001	24/10/2000	1.44		11.6	b.d.l.	b.d.l.	0.19	8.12	0.16	0.07	1.06	b.d.l.	b.d.l.	b.d.l.	0.60	18.60	b.d.l.	b.d.l.	b.d.l.	0.04	b.d.l.	b.d.l.	b.d.l.0
IRN	Louvat and Allègre, 1997	1997	1.44													0.55	19.25				0.03			
IRN	Louvat and Allègre, 1997	1997	1.58		8.1											0.55	1.44				b.d.l.			
IRN	Lopoukhine and Stieltjes, 1978	20/06/1978			18.5	b.d.l.				0.13						0.94	20.54							
IRN	Iundt et al., 1992	1992		b.d.l.	14.2	b.d.l.		b.d.l.	8.28	0.12	b.d.l.	b.d.l.	b.d.l.	b.d.l.			6.51	b.d.l.	b.d.l.		b.d.l.			b.d.l.0
MAN	Sanjuan et al., 2001	19/10/2000	4.75		7.9	0.01	b.d.l.	0.10	13.11	0.06	0.03	0.49	b.d.l.	b.d.l.	b.d.l.	0.30	9.13	b.d.l.	b.d.l.	b.d.l.	0.18	b.d.l.	b.d.l.	b.d.l.0
MAN	Louvat and Allègre, 1997	1997	4.03													0.23	7.95				0.13			
MAN	Lopoukhine and Stieltjes, 1978	24/06/1978	4.32			0.01				0.06							10.27							
MAN	Belle, 2014	01/12/2011			4.2		0.06		16.18	0.07							9.28							
MAN	Aunay et al., 2013	06/03/2012															7.91							
MAN G	Sanjuan et al., 2001	19/10/2000	2.16		4.6	b.d.l.	1.48	b.d.l.	8.85	b.d.l.	0.03	0.41	b.d.l.	b.d.l.	b.d.l.		10.16	b.d.l.	b.d.l.		0.06	b.d.l.		b.d.l.0
MANES	Sanjuan et al., 2001	24/10/2000	1.01		9.3	b.d.l.	b.d.l.	0.17	9.01	0.13	0.07	1.02	b.d.l.	b.d.l.	b.d.l.	0.47	15.64	b.d.l.	b.d.l.	b.d.l.	b.d.l.	b.d.l.	b.d.l.	b.d.l.0
MANES	Iundt et al., 1992	1992		b.d.l.	10.5	b.d.l.		b.d.l.	8.92	0.11	b.d.l.	b.d.l.	b.d.l.	b.d.l.			13.58	b.d.l.	b.d.l.		b.d.l.			b.d.l.0
MF1	Lopoukhine and Stieltjes, 1978	29/06/1978				0.02				0.03														
OLIV1	Sanjuan et al., 2001	01/10/2000	3.17		152.5	0.02	b.d.l.	b.d.l.	0.49	b.d.l.	b.d.l.	b.d.l.	b.d.l.	b.d.l.	b.d.l.		2.62	b.d.l.	b.d.l.		b.d.l.	b.d.l.		b.d.l.0
OLIV2	Sanjuan et al., 2001	26/10/2000	5.91		1992	0.04	2.97	0.62	5.70	0.01	b.d.l.	0.17	b.d.l.	b.d.l.	b.d.l.	0.82	19.86	b.d.l.	b.d.l.	b.d.l.	0.06	b.d.l.	0.01	b.d.l.0
OLIVbis	Aunay et al., 2013	12/02/2013																						
PC	Aunay et al., 2013	03/09/2012																						
PISSA	Sanjuan et al., 2001	26/10/2000	0.43		6.8	b.d.l.	b.d.l.	b.d.l.	8.86	0.04	b.d.l.	0.29	b.d.l.	b.d.l.	b.d.l.		28.42	b.d.l.	b.d.l.		b.d.l.	b.d.l.		b.d.l.0
RFOUQ	Sanjuan et al., 2001	01/10/2000	b.d.l.		0.0	b.d.l.	b.d.l.	b.d.l.	b.d.l.	b.d.l.	b.d.l.	b.d.l.	b.d.l.	b.d.l.	b.d.l.		7.30	b.d.l.	b.d.l.		b.d.l.	b.d.l.		b.d.l.0
RFOUQ	Lopoukhine and Stieltjes, 1978	25/06/1978				0.01				0.06							10.27							
sRMAT	Sanjuan et al., 2001	01/10/2000	3.75		7.3	0.01	b.d.l.	b.d.l.	0.42	b.d.l.	b.d.l.	b.d.l.	b.d.l.	b.d.l.	b.d.l.		6.05	b.d.l.	b.d.l.		0.06	b.d.l.		b.d.l.0
sRMAT2	Sanjuan et al., 2001	21/08/2000	0.14		b.d.l.	b.d.l.	b.d.l.	b.d.l.	0.25	b.d.l.	b.d.l.	0.10	b.d.l.	b.d.l.	b.d.l.		6.51	b.d.l.	b.d.l.		b.d.l.	b.d.l.		b.d.l.0
sRMAT3	Sanjuan et al., 2001	01/10/2000	1.44		7.0	0.01	1.11	b.d.l.	2.95	0.01	0.05	0.22	0.05	b.d.l.	b.d.l.		8.22	b.d.l.	b.d.l.		0.09	b.d.l.		b.d.l.0

Spring	Campaign	Date	Li (µmol/L)	Be (µmol/L)	B (µmol/L)	F (mmol/L)	Al (µmol/L)	Cr (µmol/L)	Mn (µmol/L)	Fe (mmol/L)	Co (µmol/L)	Ni (µmol/L)	Cu (µmol/L)	Zn (µmol/L)	As (µmol/L)	Rb (µmol/L)	Sr (µmol/L)	Ag (µmol/L)	Cd (µmol/L)	Cs (µmol/L)	Ba (µmol/L)	Pb (µmol/L)	U (µmol/L)	PO4 (mmol/L)
TB	Aunay et al., 2013	01/12/2012																						
TBA	Lopoukhine and Stieltjes, 1978	25/06/1978				0.02				0.06							11.41							
TBA	Aunay et al., 2013	12/03/2013																						
TR	Belle, 2014	22/11/2011			0.5		0.21		1.71	0.01							1.34							
TR	Aunay et al., 2013	08/03/2012															7.89							
VERO	Sanjuan et al., 2001	24/10/2000	0.86		7.9	b.d.l.	b.d.l.	0.15	7.17	0.11	0.05	0.95	b.d.l.	0.12	b.d.l.	0.54	14.15	b.d.l.	b.d.l.	b.d.l.	b.d.l.	b.d.l.	b.d.l.	b.d.l.0
VERO	Louvat and Allègre, 1997	1997	0.86													0.39	14.20				0.02			
VERO	Louvat and Allègre, 1997	1997	1.01		0.6											0.39	5.80				b.d.l.			
VERO	Iundt et al., 1992	1992		b.d.l.	7.9	b.d.l.		b.d.l.	6.55	0.08	b.d.l.	b.d.l.	b.d.l.	b.d.l.			9.24	b.d.l.	b.d.l.		b.d.l.			b.d.l.0

Table B.3: Literature carbon speciation and isotopic ratios in waters and gas from thermal springs of Piton des Neiges.

Spring	Source of data	pH	Temperature (°C)	TDIC (mmol/L)	H_2CO_3 (mmol/L)	HCO_3 (mmol/L)	$\delta^{13}C_{TDIC}$ (‰ PDB)	$\delta^{13}C_{CO2}$ (‰ PDB)
BACH	Marty et al., 1992	7.77	25.1	14.20	0.46	13.70	2.10	
BACH	Sanjuan et al., 2001	7.42	19.4	20.30	1.59	18.70	-1.10	
BB	Marty et al., 1992	7.22	27.6	23.09	2.29	20.80		-5.8
BB	Sanjuan et al., 2001	6.66	22.6	22.98	7.56	15.43	2.70	
BC	Marty et al., 1992	6.16	26.4	99.17	53.97	45.20		
BR14	Sanjuan et al., 2001	6.32	36.3	24.01	12.42	11.59	2.20	
GDS	Sanjuan et al., 2001	6.57	18.6	13.48	5.07	8.41	-1.40	
IRN	Marty et al., 1992	6.15	38.4	57.61	24.80	32.80	-2.30	-5.8
MAN	Marty et al., 1992	6.02	30.3	44.42	26.42	18.00		-6.7
MAN	Sanjuan et al., 2001	6.59	30.6	30.27	11.06	19.21	3.00	
MANES	Marty et al., 1992	6	31.3	64.59	38.59	26.00	-3.30	-6.3
MANES	Sanjuan et al., 2001	5.3	31	283.66	257.00	26.66	3.2000	
OLIV1	Sanjuan et al., 2001	7.26	18.9	9.21	1.01	8.20	-4.50	
OLIV2	Sanjuan et al., 2001	6.05	26	127.81	85.14	42.67	1.80	
VERO	Marty et al., 1992	6	31.6	58.97	35.07	23.90	-4.20	-6.5

C. Detail of water samples of the study area potentially depleted in heavy isotopes of oxygen and hydrogen.

Table C.1: Literature oxygen and hydrogen isotopic ratios (‰ VSMOW) for water samples used in Figure 3, collected at altitudes > 2000 m and/or associated with a cyclonic event.

Sample	Nature	Source of data	Associated with a cyclonic event	Altitude (m)	Symbol	Date	$\delta^{18}O$ (‰ VSMOW)	δD (‰ VSMOW)
Pluie Maido	Rain	Grünberger, 1989	No	2190	+	Dry season 1986	-5.4	-28.7
Pluie Maido	Rain	Grünberger, 1989	No	2190	+	Rainy season 1985-1986	-7.6	-47.0
Pluie Rivière de l'Est Haut	Rain	Nicolini, 1991	No	2250	+	1/4/1985-23/10/1985	-5.3	-19.0
Pluie Rivière de l'Est Haut	Rain	Nicolini, 1991	No	2250	+	23/10/1985-11/4/1986	-7.1	-41.3
Pluie Rivière de l'Est Haut	Rain	Nicolini, 1991	No	2250	+	11/4/1986-10/11/1986	-6.3	-32.6
Pluie Rivière de l'Est Haut	Rain	Nicolini, 1991	Yes	2250	+	10/11/1986-2/4/1987	-11.8	-78.0
Pluie Rivière de l'Est Haut	Rain	Nicolini, 1991	No	2250	+	2/4/1987-29/4/1987	-8.1	-46.1
Pluie Rivière de l'Est Haut	Rain	Nicolini, 1991	No	2250	+	29/4/1987-24/6/1987	-6.1	-29.4
Pluie Rivière de l'Est Haut	Rain	Nicolini, 1991	No	2250	+	24/6/1987-14/8/1987	-6.2	-29.6
Pluie Rivière de l'Est Haut	Rain	Nicolini, 1991	No	2250	+	14/8/1987-23/9/1987	-4.1	-14.2
Eau souterraine Le Blanchard (Trois-Bassins)	Groundwater	Aunay and Gourcy, 2007	Yes	161	×	08/03/2007	-7.7	-47.5
Ravine Trois-Bassins - RD9	Rain	Aunay and Gourcy, 2007	Yes	368	×	08/03/2007	-8.5	-57.8